

# CHAPTER 3

---

## ION EXCHANGE TECHNOLOGY

## Chapter 3

# Ion Exchange Technology

### 3.1. Introduction [14]

Ion exchange is a technology that has been ever receiving growing attention in various industries for several decades. This technology is commonly used to purify solutions by removing the dissolved ions by electrostatic sorption into ion exchange materials of various physical forms. The removed ions are replaced with equivalent amounts of other ions of the same charge in the solutions. Engineering systems of various configurations meeting the requirements for industrial application are available and vary depending on the morphology of the ion exchange materials. Batch and column systems are the most common configurations to accomplish ion exchange processes using resins, whereas plate and frame modules/cells are favoured upon using membrane/sheet forms. Currently, a large number of commercial resins and membranes are available giving high possibility for more than one technically effective solution that allows the utilization of custom-designed ion exchange process.

### 3.2. Historical Perspective

Ion exchange phenomena have been known for many years. The first examples of these phenomena were discovered by Thompson and Way (1850) during their investigations concerning the way in which soluble manures were retained for long periods in the soil, instead of being washed out by rain water. The importance of this discovery (in ion exchange terms) was not fully understood until later in that decade when this reaction was found to be reversible. This phenomenon was caused by certain minerals in the soil as released in the latter half of the nineteenth century. These minerals, called resins, are based on tetrahedron structure of silicon and aluminium compounds called zeolites. In 1905, synthetic zeolites were manufactured and utilized for water treatment in a form of water-softening agent ever since. Synthetic cation-exchange resins were developed during the 1930s using certain types of coal treated with sulphuric acid. This was an important evolution due to the fact that the sulfonated coal would operate in a greater pH range, 1–10. This made the sulfonated coal more versatile for the use in many more industrial applications. However, these resins were found to have serious deficiency caused by their lower exchange capacity compared to the zeolites. A few years later, the phenol formaldehyde polymer resin from the type shown in Fig. 3.1 was synthesized.

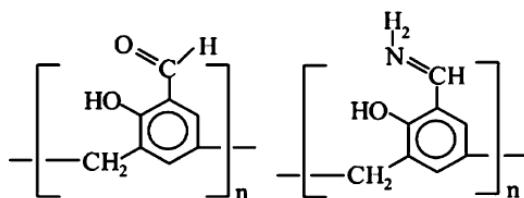


Figure 3-1 Phenol formaldehyde ion exchange resins

This polymer was sulfonated forming strong acid ion exchange resin. Using the same base polymer only functionalized with an amine (NH<sub>2</sub>) produced the first weak base ion exchange

resins. The major development for the power industry came in USA in 1944 when strong acid and strong base resins from the types shown in Fig. 3.2 were produced based on divinylbenzene cross-linked poly styrene, which was treated with sulfuric acid to make a strongly acidic resins or chloro methylated and subsequently aminated to produce strongly basic resins.

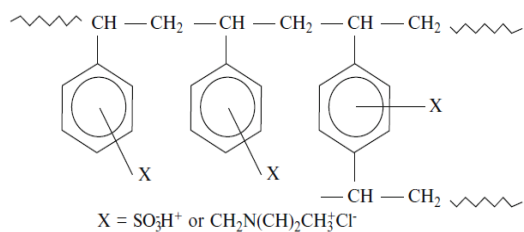


Figure 3-2 Strong cation and anion exchange resins based on polystyrene-divinylbenzene copolymer resins

These resins possess much better characteristics than earlier phenol/formaldehyde resins. These new resins are now used almost exclusively in water demineralization plants for high pressure boilers. By the year 1950, weakly acidic ion exchange resins shown in Fig.3.3 based on polymerization of methacrylic acid and divinylbenzene were developed.

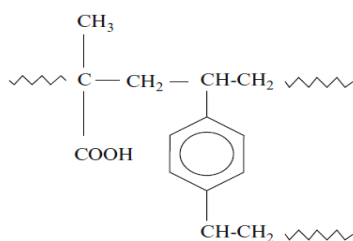
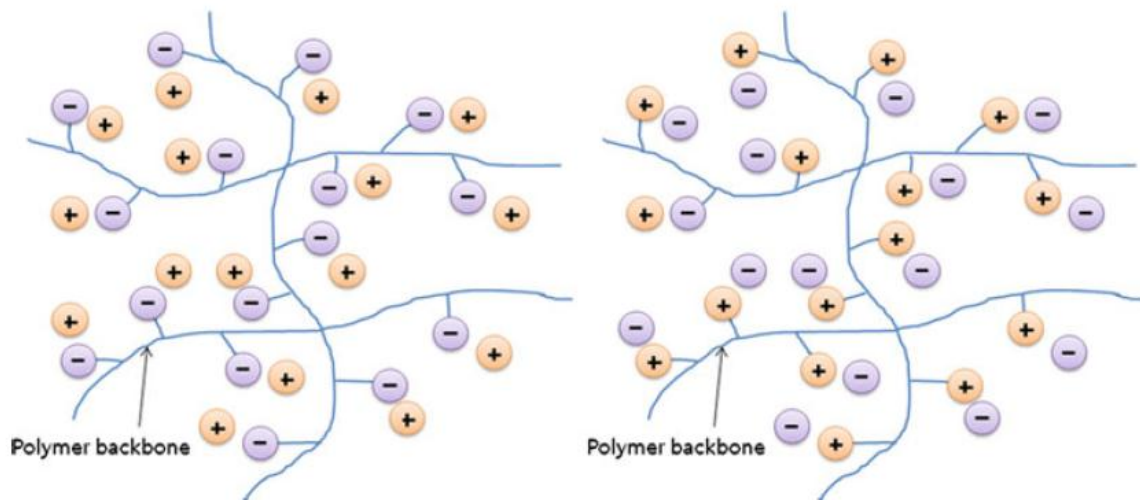


Figure 3-3 Weak cation exchange resins based on polymethylmethacrylate-divinylbenzene copolymer resins

Eventually, the macroporous methyl methacrylate and divinylbenzene resins were synthesized with various functionalities (weakly basic, strongly basic, and bipolar), by the year 1965 and above, with each resin having its own niche application in the water treatment industry

### 3.3. Structure of Ion Exchangers

An ion exchanger is an insoluble material which traps ions and simultaneously releases ions. This process is known as ion exchange reactions. The ion exchanger has a functional group. The insoluble host structure allows diffusion of hydrated ions, i.e., a hydrophilic matrix, which must carry a fixed ionic charge, termed the fixed ion. Electrical neutrality of the structure must be established by the presence of a mobile ion of opposite charge to that of the fixed ion.



**Figure 3-4 Schematic diagram of chemical structure of cation-exchangers (left) and anion-exchangers (right)**

If it has insoluble fixed anionic/cationic complement, it is a cation-/anion exchanger, respectively. In a cation-exchanger, the fixed negative charges are in electrical equilibrium with mobile cations in the interstices of the polymer as indicated in Fig. (3.4) (left-hand side), which shows schematically the matrix of a cation-exchanger with fixed anions and mobile cations; the latter are referred to as counter ions.

### 3.4. Classifications of Ion Exchange Materials

On the basis of origin, there are two general types of ion exchange materials, that is, organic and minerallic; the former majority are synthetic polymers available in cationic and anionic forms whereas the latter exists in cation-exchange form only(e.g., zeolites and betonites). Thus, organic ion exchange materials can be cationic, anionic, and combined cationic/anionic (amphoteric) exchangers considering the nature of fixed ion exchange sites (functional groups). Since ion exchangers act in a similar way to conventional acids and bases, the main classes of these materials, that is, cation and anion exchangers, can be further classified depending on the type of the functional group into several types: strongly acidic, strongly basic, weakly acidic, and weakly basic materials. Ion exchange materials containing sulfonate ( $-\text{SO}_3^-$ ) and phosphate acid ( $-\text{PO}_3^-$ ) groups and those containing tetra ammonium ( $-\text{NR}_3^+$ ) basic groups are strongly acidic and strongly basic exchangers, respectively. On the other hand, materials containing phenolic ( $-\text{OH}$ ) groups and primary amine ( $-\text{NH}_2$ ) and secondary amine ( $-\text{NRH}$ ) groups are weakly acidic and weakly basic exchangers, respectively. Carboxyl groups ( $-\text{COO}^-$ ) and tertiary amine ( $-\text{NR}_2$ ) groups take a medium position between strong and weak acidic and basic exchangers, respectively.

Practically, most strong acid exchangers contain sulfonate groups, which are active over the entire pH range. Unlikely, most weak acid exchangers have carboxylic groups, which are not active at pH values below 4–6. However, such exchangers often have higher ion exchange capacities than sulfonate exchangers together with other specific advantages. Similarly, strong basic exchangers' are active over the entire pH range unlike weak base exchangers which are not

active at alkaline pH. A summary of the common functional groups are presented in Table (3.2). It can be clearly seen that each of these major resin classes has several physical or chemical variations within the class. Such variations impart different operating properties to the resin. Thus, the terms strong and weak in the ion exchange world do not refer to the strength of binding; it rather reflects the extent of variation of ionization with pH

**Table 3-1 Common functional groups of polymeric ion exchange materials and their respective pK values**

Anion-exchange materials		Cation-exchange materials	
Fixed ionic groups	pK	Fixed ionic group	pK
$\equiv \text{N}^+$	1 -- 2	--SO <sub>3</sub> H	1 -- 2
= N	4 -- 6	--PO <sub>3</sub> H <sub>2</sub>	2 -- 5
= NH	6 --8	--COOH	4 -- 6
– NH <sub>2</sub>	8 -- 10	--OH	9 -- 10

of the medium solution. Strongly acidic resins are commonly available in Na<sup>+</sup> form or H<sup>+</sup> form with different degrees of cross-linking to meet their requirements in various applications, whereas strongly basic resins are available in Cl<sup>-</sup> or OH<sup>-</sup> forms.

Physically, organic (polymeric) ion exchange materials are available in various morphologies related to the polymer frame work carrying the functional groups. This includes beads, fibers, and membranes. Such variation in the physical forms brings about wide differences in chemical and physical properties of these ion exchangers. The majority of these ionic forms have synthetic polymer structures and mainly exist in a resin form represented by a wide number of commercial resins with polystyrene divinylbenzene backbone. A smaller class of biosorbents obtained from modified natural polymer sources including alginate, chitosan, and cellulose is also under development. Ion exchange resins fall into two main categories: cation and anion-exchange forms.

A combination of cation- and anion-exchange groups can be used to obtain a bipolar form of the resins that can replace mixed bed in ion exchange column.

Considering the separation mechanism, ion exchangers can be further classified into various categories including ion exchange resins, chelating adsorbents, hydrogels, affinity polymers, and ion exchange membranes. Among all, ion exchange resins, which are covalently cross-linked insoluble poly ions supplied as spherical beads (particles), represent the major class of exchanger being commercially produced as stated earlier.

### 3.5 Preparation of Ion Exchange Resins

Commercial ion exchange resins that are available in market today are commonly produced by suspension polymerization, poly condensation, or polymer-analogous transformations.

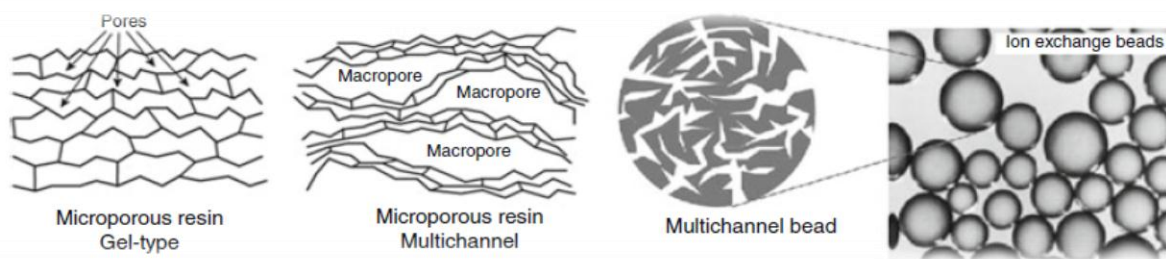


**Figure 3-5 Macroporous ion exchange resin bead with multichannel structure**

Resins based on styrene-divinylbenzene copolymers as a building block involve the preparation of a cross-linked bead copolymer followed by chemical treatment with a sulfonating agent in the case of strong acid cation exchange resins, or chloromethylation and subsequent amination of the copolymer for obtaining anion-exchange resins. The degree of cross-linking achieved in the resin beads depends on the proportions of the styrene monomer and the cross-linking agent (divinylbenzene) used in the polymerization step. Practical ranges of crosslinking are in the range of 4–16%; however, 8% cross-linking level is preferred.

It is not straight forwardly known which one of the two resin structures, that is, strongly or weakly, is advantageous without knowing specific operating conditions of the treatment site. This is because the operating properties for acrylic resins differ from those of the corresponding sulfonic acid resin. The preferred resin is the one that has operating properties matching up best with the site's operating parameters, thus maximizing operating efficiency and cost-effectiveness.

### 3.6. Physical Characteristics of Ion Exchange Resins

Physically, ion exchange beads have either a dense internal structure with no or minimal discrete pores, that is, gel (microporous) (0.5–20 nm) resins or macroporous (macroreticular) (20–200 nm) resins with multi channelled structure, as schematized in Fig. 3.5. The type of internal structure of the resins beads dictates the selection of an ion exchanger for a particular application. Macroporous resins, with their tri dimensional matrix with high effective surface area, obtained by adding porogen (phase extender) during their production followed by its washing out leaving voids in the structure, facilitate the ion exchange process. Also, multichannel structure gives an access to the exchange sites for larger ions allowing the use of almost any solvent, irrespective of whether it is a good for resin solvation together with little or no change in volume upon solvent loss. This confers more rigidity to the resin beads and facilitates their removal from the reaction system. On the other hand, the presence of no discrete pores in the microporous beads leads to a limitation in the solute ions diffusion hindering the interaction with fixed ionic sites and leading to a slowdown in the reaction rates. However, these resins offer certain advantages such as less fragility, less required care in handling, faster in functionalization and applications reactions, and possessing higher loading capacities.

Cross-linking of the resins during the preparation step is an essential step toward inheriting toughness and insolubility to the resin. The level of cross-linking plays an important role in affecting the physical and chemical properties of the resins. For example, resins with very low degree of cross-linking tend to adsorb more moisture and change dimensions markedly

depending on the type of ionic sites bound to polymer backbone. The main physical properties that get influenced by cross-linking mainly include (i) moisture content and (ii) particle size, to get it with other associated properties such as pore size and morphology, surface area, and partial volume of the resins in a swollen state. The moisture content, which is primarily a hydration of the fixed ionic groups, is a function of the degree of cross-linking and the type of functional group. Low degree of cross-linking in gel resins having sulfonic acid or quaternary ammonium groups allows absorption of large amounts of water resulting in remarkable resin swelling. Water swelling of resins leads to variation in their volume, which varies in turn with degree of hydration that depends on the attached counter (incoming) ion. However, frequent swelling and subsequent contraction during drying may shorten the resins lifetime.

On the other hand, resin particle size causes an impact on their performance. For instance; smaller particles improve the kinetics of the ion exchange reaction but cause an increase in the water pressure drop leading to a decrease of the flow rate. The chemical properties of resins involve ion exchange capacity, type of resin's matrix, and type and concentration of functional groups attached to backbone of the resin. The stability (chemical, physical, and mechanical) and the behaviour of the ion exchange resins depend primarily not only on the structure and the degree of crosslinking of the resin matrix but also on the nature and number of fixed ionic groups.

The former determines the porosity of the matrix and accordingly the degree of swelling of the resin and the mobility of the counter ions through it, which in turn controls the rates of ion exchange in the resin. Furthermore, highly cross-linked resins are harder and more resistant to mechanical breakdown but with lesser swelling and counter ion accessibility. However, higher and lower cross-linked resins are also available with less or more water sorption capabilities. Therefore, the most desired combinations of properties in ideal ion exchange resins required of industrial applications are:

- Fast kinetics, that is, speedy rate of exchange
- High chemical stability
- Physical stability in terms of mechanical strength and resistance to wear
- Reasonable degree of cross-linking
- Hydrophilic structure of regular particle size and reproducible form
- Effective and lasting ion exchange capacity
- Consistent particle size
- Effective surface area compatible with the hydraulic design requirements for large-scale plant

Finally, it can be stated that the performance of ion exchange resins in terms of kinetics and sorption equilibrium depends on the physical and chemical properties of the resins.

### **3.7. Fundamentals of Ion Exchange Reactions**

#### **3.7.1. Ion Exchange Equilibrium**

Ion exchange process depends on the mechanism by which mobile ions from an external solution are exchanged in the opposite direction for an equivalent number of ions that are electrostatically bound to the functional groups contained within a solid matrix of the ion exchange material.

The preference of one ionic species over another by the ion exchangers can be attributed to several causes:

- The electrostatic interaction between the charged frame work and the counter ions depends on the size and valence of the counter ion.
- Other effective interactions between ions and their environment.
- Large counter ions may be sterically excluded from the narrow pores of the ion exchanger.

### 3.7.1.1. Modeling of adsorption isotherm systems [15]

In general, an adsorption isotherm is an invaluable curve describing the phenomenon governing the retention (or release) or mobility of a substance from the aqueous porous media or aquatic environments to a solid-phase at a constant temperature and pH. Adsorption equilibrium (the ratio between the adsorbed amount with the remaining in the solution) is established when an adsorbate containing phase has been contacted with the adsorbent for sufficient time, with its adsorbate concentration in the bulk solution is in a dynamic balance with the interface concentration. Typically, the mathematical correlation, which constitutes an important role towards the modeling analysis, operational design and applicable practice of the adsorption systems, is usually depicted by graphically expressing the solid-phase against its residual concentration.

Its physicochemical parameters together with the underlying thermodynamic assumptions provide an insight into the adsorption mechanism, surface properties as well as the degree of affinity of the adsorbents.

- **Langmuir isotherm model**

Langmuir adsorption isotherm, originally developed to describe gas–solid-phase adsorption onto activated carbon, has traditionally been used to quantify and contrast the performance of different bio-sorbents. In its formulation, this empirical model assumes monolayer adsorption (the adsorbed layer is one molecule in thickness), with adsorption can only occur at a finite (fixed) number of definite localized sites, that are identical and equivalent, with no lateral interaction and steric hindrance between the adsorbed molecules, even on adjacent sites. In its derivation, Langmuir isotherm refers to homogeneous adsorption, which each molecule possess constant enthalpies and sorption activation energy (all sites possess equal affinity for the adsorbate), with no transmigration of the adsorbate in the plane of the surface.

Graphically, it is characterized by a plateau, an equilibrium saturation point where once a molecule occupies a site, no further adsorption can take place. Moreover, Langmuir theory has related rapid decrease of the intermolecular attractive forces to the rise of distance.

The mathematical expression of Langmuir isotherm model can be written as follows:

$$q_e = \frac{q_m K_L C_e}{1 + K_L C_e} \quad (3.1)$$

which can be linearized according to the following equation:

$$\frac{C_e}{q_e} = \frac{1}{K_L q_m} + \frac{C_e}{q_m} \quad (3.2)$$

Where  $C_e$  = the equilibrium concentration of adsorbate (mg/l),  $q_e$  = the amount of metal adsorbed per gram of the adsorbent at equilibrium (mg/g),  $q_m$  = maximum monolayer coverage capacity (mg/g),  $K_L$  = Langmuir isotherm constant (l/mg). The values of  $q_{max}$  and  $K_L$  were computed from the slope and intercept of the Langmuir plot of  $C_e/q_e$  versus  $C_e$ .

The essential features of the Langmuir isotherm may be expressed in terms of equilibrium parameter  $R_L$ , which is a dimensionless constant referred to as separation factor or equilibrium parameter can be represented as:

$$R_L = \frac{1}{1 + K_L C_0} \quad (3.3)$$

Where  $K_L$  (l/mg) is the constant related to the energy of adsorption (Langmuir Constant) and  $C_0$  is denoted to the adsorbate initial concentration (mg/l). In this context, lower  $R_L$  value reflects that adsorption is more favourable. In a deeper explanation,  $R_L$  value indicates the adsorption nature to be either unfavourable ( $R_L > 1$ ), linear ( $R_L = 1$ ), favourable ( $0 < R_L < 1$ ) or irreversible ( $R_L = 0$ ).

- **Freundlich isotherm model**

Freundlich isotherm is the earliest known relationship describing the non-ideal and reversible adsorption, not restricted to the formation of monolayer. This empirical model can be applied to multilayer adsorption, with non-uniform distribution of adsorption heat and affinities over the heterogeneous surface. Historically, it is developed for the adsorption of animal charcoal, demonstrating that the ratio of the adsorbate onto a given mass of adsorbent to the solute was not a constant at different solution concentrations. In this perspective, the amount adsorbed is the summation of adsorption on all sites (each having bond energy), with the stronger binding sites are occupied first, until adsorption energy are exponentially decreased upon the completion of adsorption process

At present, Freundlich isotherm is widely applied in heterogeneous systems especially for organic compounds or highly interactive species on activated carbon and molecular sieves.

The Freundlich isotherm can be represented by the following equation:

$$q_e = K_f C_e^n \quad (3.4)$$

Which can be linearized according to the following equation:

$$\ln q_e = \ln K_f + n \ln C_e \quad (3.5)$$

Where  $K_f$  = Freundlich isotherm constant (mg/g),  $n$  = adsorption intensity;  $C_e$  = the equilibrium concentration of adsorbate (mg/l).  $q_e$  = the amount of metal adsorbed per gram of the adsorbent at equilibrium (mg/g). The constant  $K_f$  is an approximate indicator of adsorption capacity. The values of  $K_f$  and  $n$  can be computed by plotting  $\ln q_e$  versus  $\ln C_e$ . The slope ( $n$ ) ranges between 0 and 1 is a measure of adsorption intensity or surface heterogeneity, becoming more heterogeneous as its value gets closer to zero. Whereas, a value below unity implies chemisorptions process, while  $1/n$  is a function of the strength of adsorption in the adsorption process. If  $n = 1$  then the partition between the two phases are independent of the concentration. If value of  $1/n$  is below one it indicates a normal adsorption. On the other hand,  $1/n$  being above one indicates cooperative adsorption. [16]

- **Temkin isotherm model**

Temkin isotherm is the early model describing the adsorption of hydrogen onto platinum electrodes within the acidic solutions. The isotherm contains a factor that explicitly taking into the account of adsorbent–adsorbate interactions. By ignoring the extremely low and large value of concentrations, the model assumes that heat of adsorption (function of temperature) of all molecules in the layer would decrease linearly rather than logarithmic with coverage. As implied in the equation, its derivation is characterized by a uniform distribution of binding energies (up to some maximum binding energy). Temkin equation is excellent for predicting the gas phase equilibrium (when organization in a tightly packed structure with identical orientation is not necessary), conversely complex adsorption systems including the liquid-phase adsorption isotherms are usually not appropriate to be represented. Temkin isotherm model can be expressed as follows:

$$q_e = \frac{RT}{b_T} \ln A_T + \frac{RT}{b_T} \ln(C_e) \quad (3.6)$$

$$\text{Where } B = \frac{RT}{b_T} \quad (3.7)$$

$A_T$  = Temkin isotherm equilibrium binding constant (l/g),  $b_T$  = Temkin isotherm constant,  $R$  = universal gas constant (8.314J/mol.K),  $T$  = Temperature at 298K,  $B$  = Constant related to heat of sorption (J/mol)

Temkin isotherm, which considers the effects of the heat of adsorption that, decreases linearly with coverage of the adsorbate and adsorbent interactions [16].

### 3.7.1.2. Error Functions: [15]

Within recent decades, linear regression has been one of the most viable tool defining the best-fitting relationship quantifying the distribution of adsorbates, mathematically analyzing the adsorption systems and verifying the consistency and theoretical assumptions of an isotherm model. Due to the inherent bias resulting from the transformation which riding towards a diverse form of parameters estimation errors and fits distortion, several mathematically rigorous error functions such as Hybrid fractional error function, nonlinear chi-square test.

- **Hybrid Fractional Error Function (HYBRID)**

The error function was developed to improve Sum square error ERRSQ (which the most widely used error function, at higher end of the liquid-phase concentration ranges) fit at low concentrations. Hereby, each ERRSQ value is divided by the experimental solid-phase concentration with a divisor included in the system as a term for the number of degrees of freedom (the number of data points minus the number of parameters within the isotherm equation). The HYBRID fractional error function can be calculated from the following equation:

$$\text{HYBRID} = \frac{(q_{e,\text{exp}} - q_{e,\text{cal}})^2}{q_{e,\text{exp}}} \quad (3.8)$$

- **Nonlinear Chi-Square Test ( $X^2$ )**

Nonlinear chi-square test is a statistical tool necessary for the best fit of an adsorption system, obtained by judging the sum squares differences between the experimental and the calculated data, with each squared difference is divided by its corresponding value (calculated from the models). Small  $X^2$  value indicates its similarities while a larger number represents the variation of the experimental data. The nonlinear Chi-Square test can be expressed by the following equation:

$$X^2 = \sum \frac{(q_{e,exp} - q_{e,cal})^2}{q_{e,cal}} \quad (3.9)$$

### 3.7.2. Ion Exchange Kinetics [14]

Kinetics of the ion exchange reaction represents the speed with which reaction takes place. Upon designing an ion exchange process system, the rate of exchange, which is subjected to mass-transfer resistances in both liquid and solid phases, is highly significant in the design and operation of the ion exchange process. The exchange rate has impact on the size of the ion exchange columns required and/or its flow rate. The kinetics of the ion exchange reaction is affected by the type and nature of the exchanger, solution concentration, and temperature at which the exchanger is operated. When an ion exchange bead is brought into contact with a solution, a static liquid film of a thickness varying in the range of 10–100 nm depending on the rate of flow of liquid passes the particle, is formed around it. The ion exchange process taking place between the resin particle and the solution involves six distinct steps; any combination thereof can be the rate controlling step. They are:

- Diffusion of counter ions through the bulk solution surrounding the bead
- Diffusion of counter ions through the hydrated film of solution that is in close contact with the bead matrix (film diffusion)
- Diffusion of counter ions within the bead matrix (interapartical diffusion)
- The actual ion exchange reaction
- Diffusion of the exchanged species out of the ion exchange bead
- Diffusion of the exchanged species from the bead surface particle into the bulk solution

It is noteworthy mentioning that the concentration differences that might occur in the bulk solution are constantly leveled out by agitation, which disturbs the necessary transfer by convection. Nonetheless, agitation neither affects the interior of the beads nor the thin liquid film, which adheres to the bead surfaces.

The ion transfer takes place within the beads and through the thin film only by molecular diffusion, and as a result, the actual ion exchange reaction occurs very quickly and is not generally considered to be rate limiting. Thus, the rate-determining step is either the inter diffusion of counter ions within the ion exchanger itself (particle diffusion) or inter diffusion of counter ions in the adherent film (film diffusion).

In practice, either step can be the rate-determining step. However, the slower of these two steps controls the overall reaction rate. In intermediate cases, the rate may be affected by both steps. Moreover, the particle size of the resin being used is also a determining factor. Uniform particle-sized resins exhibit enhanced kinetic performance compared to conventional poly dispersed

resins due to the absence of kinetically slow larger beads. Recent studies showed that ion exchange resins in fibrous forms have improved the kinetics allowing greater adsorption of toxic and precious metals.

It is important to mention that in systems with ion exchange through organic solvents, the transfer of the counter ions in the resin is usually lower than in aqueous systems because swelling is less pronounced and electrostatic interactions with the fixed charges are stronger. Particle diffusion, thus, is relatively slow and, hence, usually controls the rate-controlling mechanism. Finally, the actual rates of ion exchange can vary over a wide range, requiring a few seconds to several months to reach equilibrium.

- **Intraparticle Diffusion Model**[17]

The most commonly used technique for identifying the mechanism involved in the adsorption process is by fitting an intraparticle diffusion plot. The intraparticle diffusion model is expressed by the following equation:

$$q_t = k_i t^{1/2} + c \quad (3.10)$$

where  $q_t$  (mg/g) is the amount of metal ion adsorbed at time  $t$  (min) and  $k_i$  is intraparticle diffusion rate constant (mg/(g min<sup>1/2</sup>)),  $c$  is the intercept of intraparticle diffusion stage.

According to this model, the plot of uptake,  $q_t$ , versus the square root of time ( $t^{1/2}$ ) should be linear if intra-particle diffusion is involved in the adsorption process and if these lines pass through the origin then intra-particle diffusion is the rate-controlling step. When the plots do not pass through the origin, this is indicative of some degree of boundary layer control and this further show that the intra-particle diffusion is not the only rate-limiting step, but also other kinetic models may control the rate of adsorption, all of which may be operating simultaneously.

### 3.7.2.1. Adsorption Kinetic Models

- **Pseudo-first-order Rate Equation** [18]

Lagergren (1898) presented a first-order rate equation to describe the kinetic process of liquid-solid phase adsorption of oxalic acid and malonic acid onto charcoal, which is believed to be the earliest model pertaining to the adsorption rate based on the adsorption capacity. It can be presented as follows:

$$\frac{dq_t}{dt} = k_1 (q_e - q_t) \quad (3.11)$$

Where  $q_e$  and  $q_t$  (mg/g) are the adsorption capacities at equilibrium and time  $t$  (min), respectively.  $k_1$  (min<sup>-1</sup>) is the pseudo-first-order rate constant for the kinetic model. Integrating Eq.(3.14) with the boundary conditions of  $q_t=0$  at  $t=0$  and  $q_t=q_t$  at  $t=t$ , yields

$$\log (q_e - q_t) = \log (q_e) - \left( \frac{k_1}{2.303} \right) t \quad (3.12)$$

To distinguish kinetic equations based on adsorption capacity from solution concentration, Lagergren's first order rate equation has been called pseudo-first-order. In recent years, it has been widely used to describe the adsorption of pollutants from wastewater in different fields,

such as the adsorption of methylene blue from aqueous solution by broad bean peels and the removal of malachite green from aqueous solutions using oil palm trunk fibre

- **Pseudo-second-order Rate Equation** [19]

If the rate of sorption is a second order mechanism, the pseudo second order chemisorption kinetic rate equation is expressed as follows:

$$\frac{dq_t}{dt} = k_2 (q_e - q_t)^2 \quad (3.13)$$

Where  $q_e$  and  $q_t$  are the sorption capacity at equilibrium and at time  $t$ , respectively ( $\text{mg g}^{-1}$ ) and  $k_2$  is the rate constant of pseudo-second order sorption ( $\text{gmg}^{-1} \text{min}^{-1}$ ). For the boundary conditions  $t=0$  to  $t = t$  and  $q_t =0$  to  $q_t = q_t$ , the integrated form of Eq. (3.13) becomes:

$$\frac{1}{q_e - q_t} = \frac{1}{q_e} + k_2 t \quad (3.14)$$

Which is the integrated rate law for a pseudo-second order reaction. Eq. (3.14) can be rearranged to obtain a linear form:

$$\frac{t}{q_t} = \frac{1}{k_2 q_e^2} + \left( \frac{1}{q_e} \right) t \quad (3.15)$$

Where  $h$  can be regarded as the initial sorption rate as  $t =0, q_t =0$  hence:

$$h = k_2 q_e^2 \quad (3.16)$$

Eq. (3.17) can be written as:

$$\frac{t}{q_t} = \frac{1}{h} + \left( \frac{1}{q_e} \right) t \quad (3.17)$$

- **Elovich's Equation** [18]

A kinetic equation of chemisorption was established by Zeldowitsch (1934) and was used to describe the rate of adsorption of carbon monoxide on manganese dioxide that decreases exponentially with an increase in the amount of gas adsorbed, which is the so-called Elovich equation in a linear form Elovich equation can be expressed as:

$$q_t = \frac{\ln a_e b_e}{b_e} + \frac{1}{b_e} \ln t \quad (3.18)$$

Where ( $a_e$ ) is the initial adsorption rate ( $\text{mg g}^{-1} \text{min}^{-1}$ ), and the parameter ( $b_e$ ) is related to the extent of surface coverage and activation energy for chemisorption. The values of  $a_e$ , and the desorption constant, ( $b_e$ ), were calculated from the intercept and slope of the straight-line plots of  $q_t$  against  $\ln t$ . Elovich's equation has been widely used to describe the adsorption of gas onto solid systems. Recently it has also been applied to describe the adsorption process of pollutants from aqueous solutions. Elovich model basically supports chemisorptions.

Elovich equation is also used successfully to describe second order kinetic assuming that the actual solid surfaces are energetically heterogeneous, but the equation does not propose any definite mechanism for adsorbate-adsorbent.

### 3.7.3. Ion Exchange Capacity [14]

Capacity of the ion exchange materials is a significant chemical characteristic that is defined as the number of counter ion equivalents that can be adsorbed in a specified amount of ion exchange material. The ion exchange capacity and related data are primarily used for (i) describing the total available exchange capacity of ion exchange materials and (ii) the use in the numerical predesign calculations of ion exchange processes. This value is expressed in milliequivalents per gram (meq/g) or milliequivalents per milliliter (meq/mL) based on the dry and wet weights of the material in a given form ( $H^+$  or  $Cl^-$ ), respectively. The capacity of the resins can be described in various ways depending on the conditions.

For example, maximum ion exchange capacity (meq/g dry  $H^+$  or  $Cl^-$  form) is represented by the total static exchange capacity when it is determined under static conditions, whereas the dynamic or volume-exchange capacity (eq/l packed bed in  $H^+$  or  $Cl^-$  form and fully water-swollen) is determined by passing a solution through a bed of the exchanger. The extent of the use of the total exchange capacity depends on the level of ionization of the functional groups of the exchanger together with the chemical and physical conditions of the process. The total dynamic capacity can be also expressed as breakthrough capacity, which characterizes the column operation and depends on (i) column design and operating parameters, (ii) the concentration of the ions being removed, and (iii) the effects of interference from other competing ions.

When ion exchangers are in a resin form, the separation is conventionally accomplished by either batch or column method.

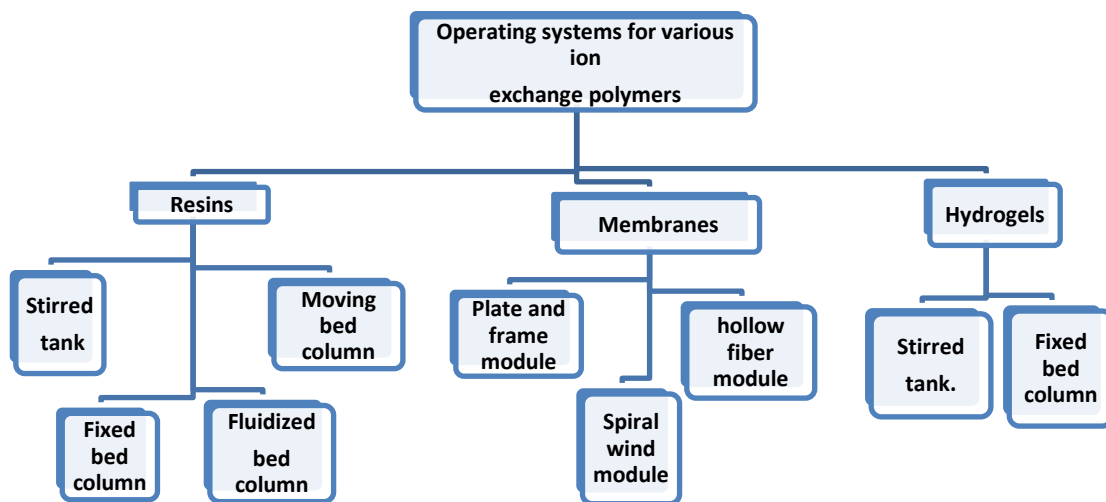


**Figure 3-6 various operating configurations for different morphologies of ion exchange materials**

### 3.8. Operating Configurations of Ion Exchange Processes using Resins

Upon utilization of ion exchange process, solution (influent) is pumped through a vessel loaded with the ion exchange resin and represents one of four basic operating configurations (1) continuous stirred (batch) tank, (2) fixed bed column, (3) fluidized bed column, and (4) a moving bed (closed loop) system.

### 3.8.1 Continuous Stirred Batch Tank [20]

In a batch method, the resin and solution are mixed in a batch tank, the exchange reaction is allowed to come to equilibrium, and then the resin is separated from the solution. The degree to which the exchange takes place is limited by the preference the resin exhibits for the target ions in solution. Consequently, the use of the resin's exchange capacity is limited unless the selectivity for the ions in solution is far greater than for the exchangeable ion attached to the resin. Because batch regeneration of the resin is chemically inefficient, batch processing by ion exchange has limited potential for industrial applications and often used in laboratories for fundamental sorption equilibrium and kinetic studies.

The dimensions of the liquid content of a vessel and the dimensions and arrangement of impellers, baffles and other internals are factors that influence the amount of energy required for achieving a needed amount of agitation or quality of mixing. The internal arrangements depend on the objectives of the operation: whether it is to maintain homogeneity of a reacting mixture or to keep a solid suspended or a gas dispersed or to enhance heat or mass transfer. a basic range of design factors, however, can be defined to cover the majority of cases, for example as in figure(3.7) which represents a basic stirred tank design.

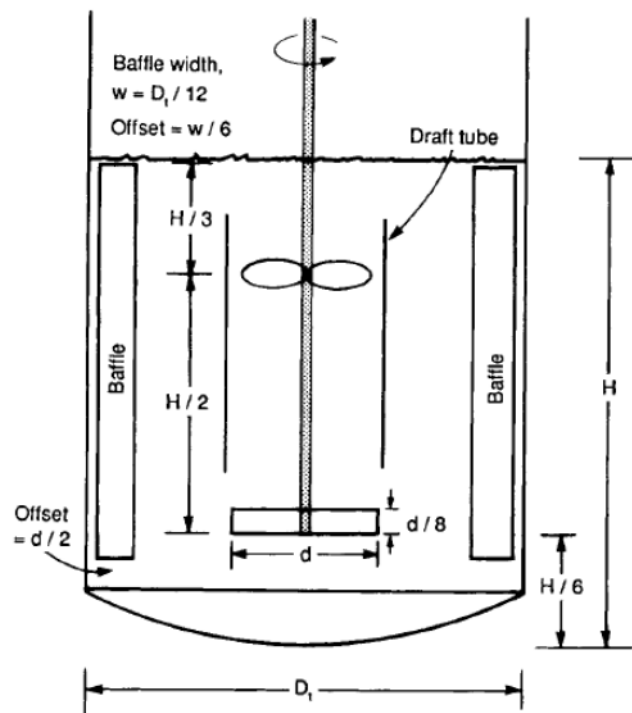


**Figure 3-7 A basic stirred tank design, not to scale, showing a lower radial impeller and an upper axial impeller housed in a draft tube. Four equally spaced baffles are standard. (  $H$  = height of liquid level,  $D$ , = tank diameter,  $d$  =impeller diameter).**

#### 3.8.1.1. Impellers [21, 22]

Impeller agitators are divided into two classes: those that generate currents parallel with the axis of the impeller shaft and those generate currents in a tangential or radial direction. The first are

called axial flow impellers, the second radial flow impellers. The three main types of impellers are propellers, paddles, and turbines which will be discussed in the next section.

### A. Propellers

A propeller is an axial flow, high speed impeller for liquids of low viscosity. The flow currents leaving the impeller continue through the liquid in a given direction until deflected by the floor or wall of the vessel. Because of the persistence of the flow currents, propeller agitators are effective in very large vessels. A typical propeller is illustrated in figure (3.8). Standard three bladed marine propellers with square pitch are most common, four bladed toothed, and other designs are employed for special purposes. Propellers rarely exceed 18 in. in diameter regardless of the size of the vessel. In a deep tank two or more propellers may be mounted on the same shaft, usually directing the liquid in the same direction. Sometimes two propellers work in opposite directions, or in “push-pull”, to create a zone of especially high turbulence between them.

For the simpler problems an effective agitator consists of a flat paddle turning on a vertical shaft. Sometimes the blades are pitched, more often they are vertical. Paddles turn at slow to moderate speeds in the center of a vessel; they push the liquid radially and tangentially with almost no vertical motion at the impeller unless the blades are pitched. The currents they generate travel outward to the vessel wall and then either upward or downward. In deep tanks several paddles are mounted one above the other on the same shaft. In some designs the blades conform to the shape of a dished or hemispherical vessel so that they scrape the surface or pass over it with close clearance. A paddle of this kind is known as an anchor agitator and is illustrated in figure (3.9). Anchors are useful for preventing deposits on a heat transfer surface, as in a jacketed process vessel, but they are poor mixers. They nearly always operate in conjunction with a higher speed paddle or other agitators, usually turning in the opposite direction.

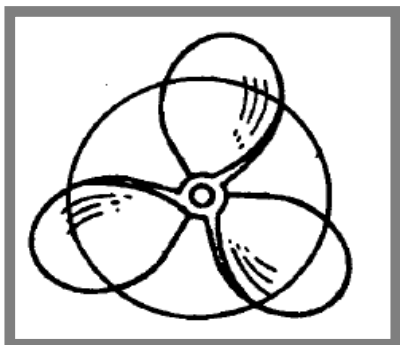


Figure 3-8 Three blade marine propeller

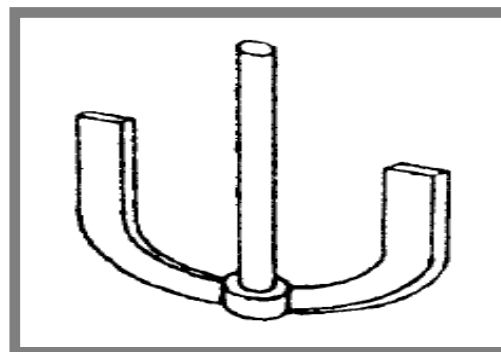


Figure 3-9 Anchor paddles

### B. Turbines

Some of the many designs of turbine are shown in figure (3.10). Most of them resemble multibladed paddle agitators with short blades, turning at high speeds on a shaft mounted centrally in the vessel. The blades may be straight or curved, pitched or vertical. The diameter of

the impeller is smaller than with paddles, ranging from 30 to 50 percent of the diameter of the vessel.

Turbines are effective over a very wide range of viscosities. In low viscosity liquids turbines generate strong currents that persist throughout the vessel, seeking out and destroying stagnant pockets. Near the impeller is a zone of rapid currents, high turbulence, and intense shear. The principle currents are radial and tangential. The tangential components induce vortexing and swirling, which must be stopped by baffles or by a diffuser ring if the impeller is to be most effective.

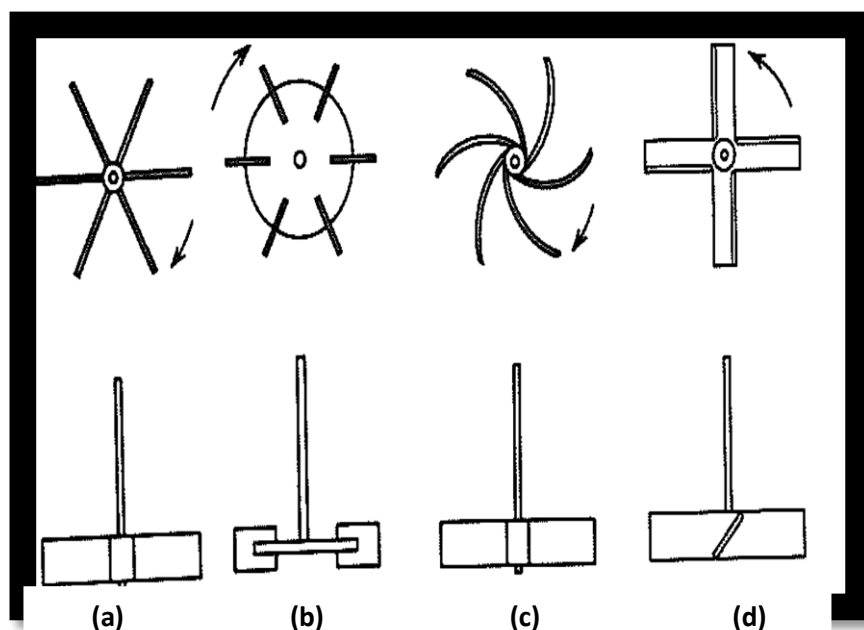


**Figure 3-10 Different designs of turbine impeller (a) open straight six blade turbine, (b) bladed disk turbine, (c) vertical curved blade turbine, (d) pitched blade turbine**

### 3.8.2. Fixed Bed Column: [14]

The fixed bed column operation is the most usable ion exchange configuration in industrial applications. It has a basic component of which the bead column is considered to be analogous of several batch reactors in series. The purpose of the column operation is to work around the limitation of selectivity of the resin. To favour high selectivity, more stages can be used (multi column system). Three types of column operation modes are available: (1) down flow, (2) up flow, and (3) counter flow. Most column beds operate with down flow operation, as shown in Fig. (3.11) that depict a schematic representation of fixed bed ion exchange column system with operation and regeneration modes. This is where feed pass down through the resin bed. On the contrary, up flow operation is used when the feed is raised through a bed. The final flow is

counter flow, and it consists of the feed flowing down from the top and the regenerate flows up from the bottom.

Most industrial applications of ion exchange use fixed bed column systems, the basic component of which is the resin column. Ion exchange column is typically applied in a pressure vessel, as shown in Fig. (3.12). It is equipped with appropriate internal plumbing that has two purposes:

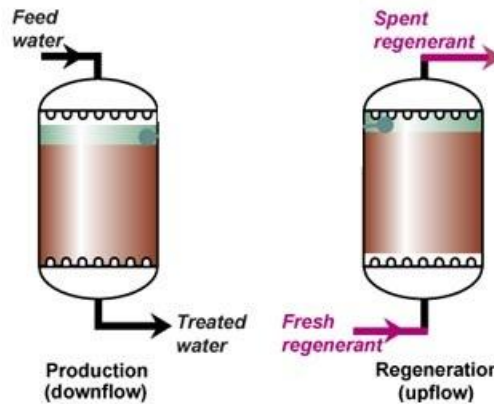


Figure 3-11 Schematic representation of fixed bed ion exchange column system showing operation and regeneration modes

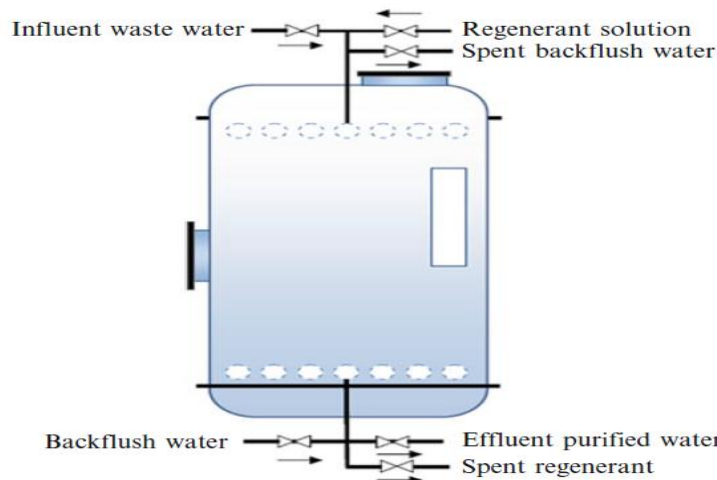


Figure 3-12 Typical structure of ion exchange column.

(i) It prevents the ion exchange resin from being washed out of the vessel and (ii) it provides an appropriate distribution of liquid flow through the ion exchange resin bed. The internal system is a corrosion-resistant screen mounted above a porous backing plate. The pressure vessel is also equipped with slit nozzles (strainers), piping, and fittings to maintain low pressure drop. During the operation, the pressure vessel is filled to only half of its volume with the empty space above the ion exchange resin bed (called free board) to allow free volume for swelling and shrinking during operations of exhaustion and regeneration.

In summary, the column design must consider the following:

- Contain and support the ion exchange resin.
- Uniformly distribute the service and regeneration flow through the resin bed.
- Provide space to allow the resins to swell, shrink, and be fluidized during backwash.
- Include the piping, valves, and instruments needed to regulate flow of feed, regenerant, and backwash solutions.

### 3.8.2.1 Column Bed Operation

In column operation, the total capacity or breakthrough capacity generally refers to the volume of the solution that can be treated before a sharp increase in the effluent concentration of the ionic species being removed is observed. At this point, the ion exchange medium is considered to be exhausted and must be replaced or regenerated. This trend can be clearly seen in the column schematic representation shown in Fig. (3.13). Part I refers to the resin, which has finished exchange reaction; part II refers to the exchange zone in the resin, which is working until it moves downward with the continuous flow of Y ions (ion to be removed); and part III represents the zone in which the resin is exhausted and Y ions completely breakthrough the resins.

Thus, the performance of ion exchanger is measured by comparing the solution concentration or conductivity of both influent and effluent, which can be monitored in terms of ion-exchanger effectiveness known as decontamination factor (DF), which is defined as a ratio of the concentration (or activity) of the fluid at the inlet compared to the concentration (or activity) at the effluent (Eq. 3.19), which expresses the effectiveness of an ion exchange process.

$$DF = \frac{\text{Influent concentration or conductivity}}{\text{Effluent concentration or conductivity}} \quad (3.19)$$

In practice, the operator of the ion exchange system has to have a certain required value for DF. For example, if the decontamination factor requirement is 100, the ion exchange bed has to be replaced when 1% breakthrough occurs. Therefore, the breakthrough capacity is practically the most interesting parameter in the design of a column type ion exchange system and is generally given as the number of bed volumes (the ratio of the volume of the liquid processed before the breakthrough point to the volume of the settled bed of the exchanger).

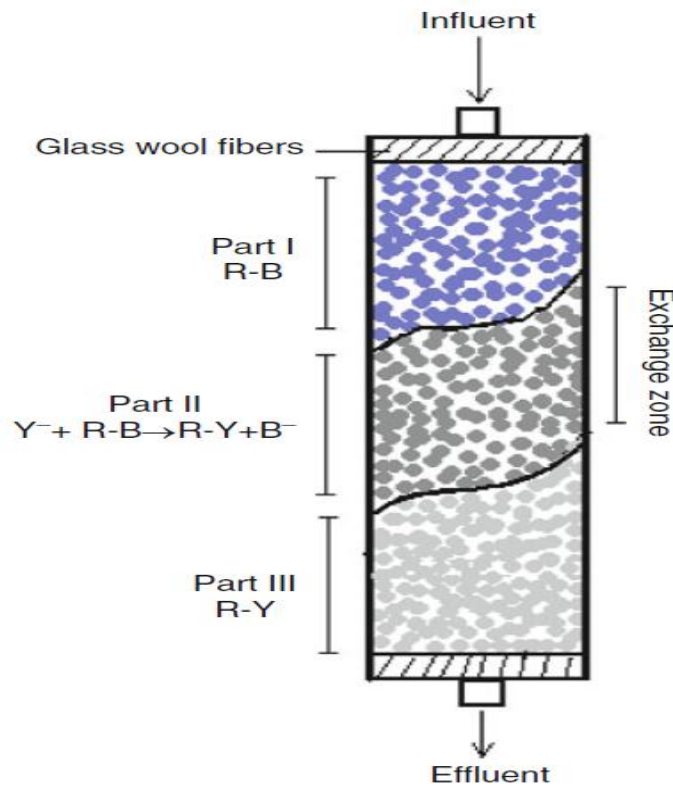


Figure 3-13 Schematic diagram of ion exchange column

A typical breakthrough curve is shown in Fig.(3.14). The points  $C_o$  and  $C_x$  are the concentrations of  $Y^-$  in the influent and effluent, respectively. The breakthrough begins at point c, and the extent of breakthrough increases until point e (end point) beyond which no further ion exchange takes place (i.e., a complete exhaustion point of the column). The breakthrough capacity is proportional to the area (abcd) and so is the overall capacity to the area (aecd). The shape of the breakthrough curve and the breakthrough capacity (i.e., the total liquid volume treated up to a particular percentage breakthrough) depend on the operating parameters.

Some important parameters that affect the breakthrough capacity include:

- The nature of the functional group on the exchanger
- The ion exchange medium grain size
- The degree of cross-linking of the resins
- The concentration and type of ions in the solution to be treated
- The flow rate of the feed solution
- The rate of percolation
- Depth of the resin bed
- Type, concentration, and quantity of regenerant

In practical operations, it is desirable to have the breakthrough curve as steep as possible to increase the extent of column utilization (i.e., bringing the ratio of the breakthrough capacity to the total capacity closer to unity).

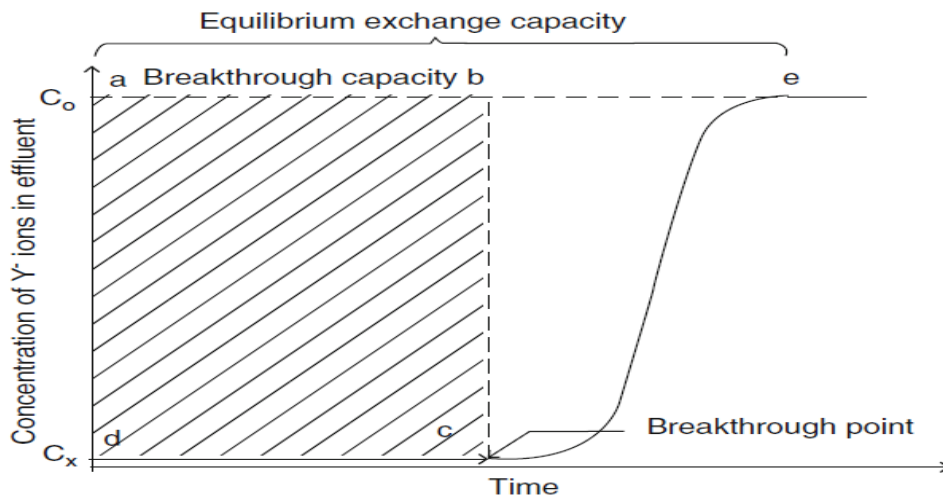


**Figure 3-14 Schematic representation of breakthrough curve**

It is worth noting that upon requirement of high DF, the degree of column utilization can vary considerably for different ion exchange resins.

### 3.8.2.2. Breakthrough Curve Modeling [3]

Successful design of an ion exchange column requires prediction of the breakthrough curve for the effluent. Over the years, several simple mathematical models have been developed for describing and analyzing the lab-scale column studies for the purpose of industrial applications. So in this study, Adams–Bohart, Thomas–Yoon models were developed to identify the best model for predicting the dynamic behavior of the column.

- **Adams–Bohart Model**

Bohart and Adams Model was based on the surface reaction theory which established a fundamental equation, which describes the relationship between  $C_t/C_0$  and  $t$  in a continuous system. This model assumes that that equilibrium is not instantaneous. It is used for describing the initial part of the breakthrough curve. The model expression is as follows:

$$\ln \left( \frac{C_t}{C_0} \right) = k_{AB} C_0 t - k_{AB} N_0 \left( \frac{Z}{U_0} \right) \quad (3.20)$$

Where  $C_0$  and  $C_t$  are the influent and effluent concentration (mg/l), respectively;  $k_{AB}$  is the kinetic constant (l/mg min),  $N_0$  is the saturation concentration (mg/l),  $Z$  is the bed depth of the fix-bed column (cm) and  $U_0$  is the superficial velocity (cm/min) defined as the ratio of the volumetric flow rate  $Q$  ( $\text{cm}^3/\text{min}$ ) to the cross-sectional area of the bed  $A$  ( $\text{cm}^2$ ). The range of  $t$  was taken into consideration from the beginning to the end of breakthrough .The parameters  $k_{AB}$  and  $N_0$  can be calculated from the linear plot of  $\ln(C_t/C_0)$  against  $t$  .

- **Thomas Model:**

Thomas model assumes plug flow behavior in the bed. This model is one of the most general and widely used to describe the performance theory of the sorption process in fixed-bed column. The linearized form of this model can be described by the following expression:

$$\ln\left(\frac{C_o}{C_t} - 1\right) = \frac{k_{Th}q_o w}{Q} - k_{Th}C_o t \quad (3.21)$$

Where  $k_{Th}$  is the Thomas model constant (mL/min mg),  $q_o$  is the adsorption capacity (mg/g), and  $t$  stands for total flow time (min). The values of  $k_{Th}$  and  $q_o$  can be determined from the linear plot of  $\ln[(C_o/C_t) - 1]$  against  $t$ .

- **Yoon–Nelson Model:**

Yoon and Nelson developed a model to investigate the breakthrough behavior of adsorbate gases on activated charcoal. The Yoon–Nelson model is based on the assumption that the rate of decrease in the probability of adsorption for each adsorbate molecule is proportional to the probability of adsorbate adsorption and the probability of adsorbate breakthrough on the adsorbent. The linearized Yoon–Nelson model for a single component system can be expressed as:

$$\ln\left(\frac{C_t}{C_o - C_t}\right) = k_{YN}t - k_{YN}\tau \quad (3.22)$$

Where  $k_{YN}$  is the rate constant (min<sup>-1</sup>) and  $\tau$  is the time required for 50% adsorbate breakthrough (min). A linear plot of  $\ln[C_t/(C_o - C_t)]$  against  $t$  determined the values of  $k_{YN}$  and  $\tau$  from the intercept and slope of the plot.

- **The Standard Error [23]**

The standard error (SE) values were determined for the adsorption capacity obtained by Thomas and Yoon-Nelson model:

$$SE = \sqrt{\sum \frac{(q_{o_{exp}} - q_{o_{cal}})^2}{N}} \quad (3.23)$$

Where,  $q_{o_{exp}}$  is experimental adsorption capacity,  $q_{o_{cal}}$  is adsorption capacity calculated using theoretical kinetic models and  $N$  is the number of experimental run points.

- **Bed depth Service Time (BDST) Model [24]**

The BDST is a model for predicting the relationship between bed depth,  $Z$  and service time. This model is used only for the description of the initial part of the breakthrough curve i.e. up to the breakpoint or 10–50% of the saturation points. This BDST model was focused on the estimation of characteristic parameters such as the maximum adsorption capacity and kinetic constant. The original BDST model was carried out by Bohart and Adams and given in the following Eq.:

$$\ln\left(\frac{C_o}{C_b} - 1\right) = \ln\left(\exp\left(\frac{KN_o Z}{v}\right) - 1\right) - KC_o t \quad (3.24)$$

A linear relationship between the bed depth and service time by rearranging as Eq. (3.25)

$$t_b = \frac{N_o Z}{C_o v} - \frac{1}{K C_o} \ln\left(\frac{C_o}{C_b} - 1\right) \quad (3.25)$$

Where  $t_b$  is service time at breakthrough point;  $N_o$  is adsorption capacity per volume of bed (mg cm<sup>-3</sup>),  $Z$  is the depth of adsorbent bed (cm),  $C_o$  is influent or initial solute concentration (mg l<sup>-1</sup>),

$v$  is linear flow rate ( $\text{cm h}^{-1}$ ),  $K$  is rate constant of adsorption ( $\text{mg}^{-1} \text{h}^{-1}$ ) and  $C_b$  is the effluent concentration at breakthrough point ( $\text{mg l}^{-1}$ ).

The critical bed depth ( $Z_0$ ) is the theoretical depth of adsorbent sufficient to ensure that the outlet solute concentration does not exceed the breakthrough concentration ( $C_b$ ) value at time  $t=0$ , when  $\exp\left(\frac{KN_0Z}{v}\right) \gg 1$ , and solving Eq.(3.25),  $Z_0$  can be calculated from the following equation.

$$Z_0 = \frac{v}{KN_0} \ln\left(\frac{C_0}{C_b} - 1\right) \quad (3.26)$$

At 50% of breakthrough, the logarithmic term in Eq. (3.26) reduces to zero, and the final term in the BDST equation become zero, giving the relationship as Eq. (3.27).

$$t_{50} = \frac{N_0}{C_0 v} Z \quad (3.27)$$

### 3.8.3. Moving Bed Reactor [25]

A moving bed is a vessel where solid particles (either reactant or catalyst) are continuously fed and withdrawn as shown in figure (3.15). The gas flow is maintained to allow the downward movement of the particles.

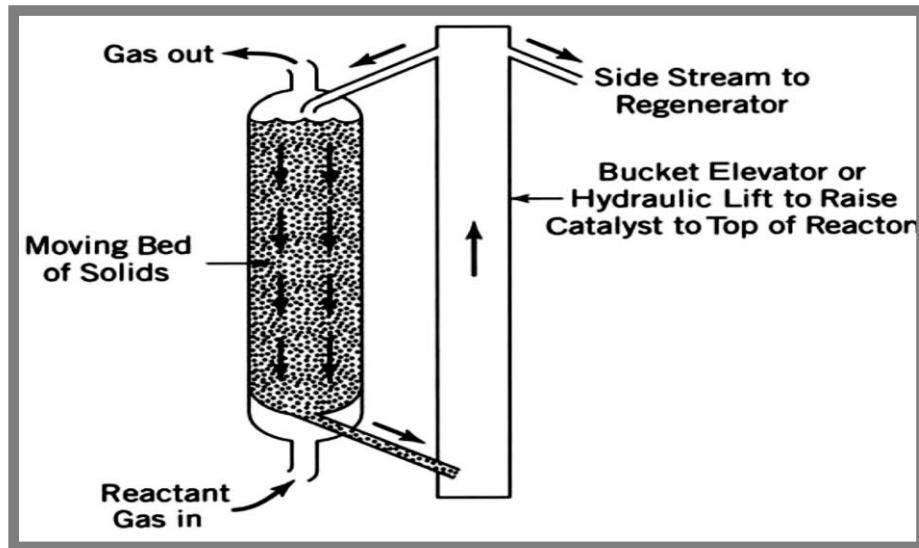


Figure 3-15 Moving bed reactor

### 3.8.4 Fluidized Bed Reactors [25,26]

The essential feature of a fluidized bed reactor is that the solids are held in suspension by the upward flow of the reacting fluid as shown in figure (3.16), this promotes high mass and heat transfer rates and good mixing. Heat transfer coefficients in the order of  $200 \text{ W/m}^2 \text{ }^\circ\text{C}$  to jackets and internal coils are typically obtained. The solids may be a catalyst, a reactant in fluidized combustion processes, or an inert powder, added to promote heat transfer. Fluidization can only be used with relatively small sized particles,  $<300 \text{ }\mu\text{m}$  with gases.

Advantages of Fluidized Bed over Fixed Bed:

- i- High rate of heat transfer.
- ii- Fluidized beds are also useful where it is necessary to transport large quantities of solids as part of the reaction processes, such as where catalysts are transferred to another vessel for regeneration.

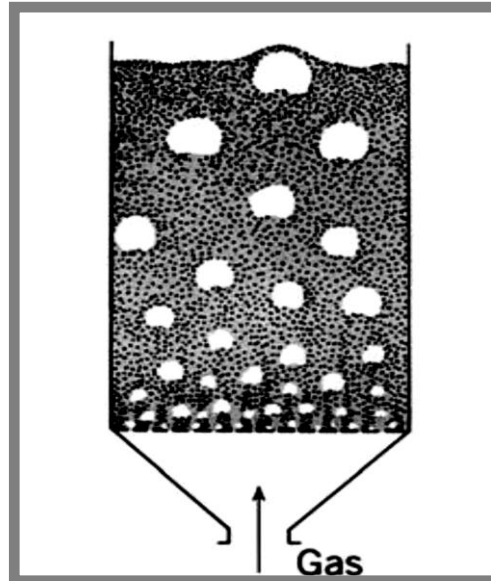


Figure 3-16 Fluidized bed reactor

### 3.9. Cycle of Ion Exchange Column Process [14]

When ion exchangers are in a resin form, the separation is conventionally accomplished by either batch or column method.

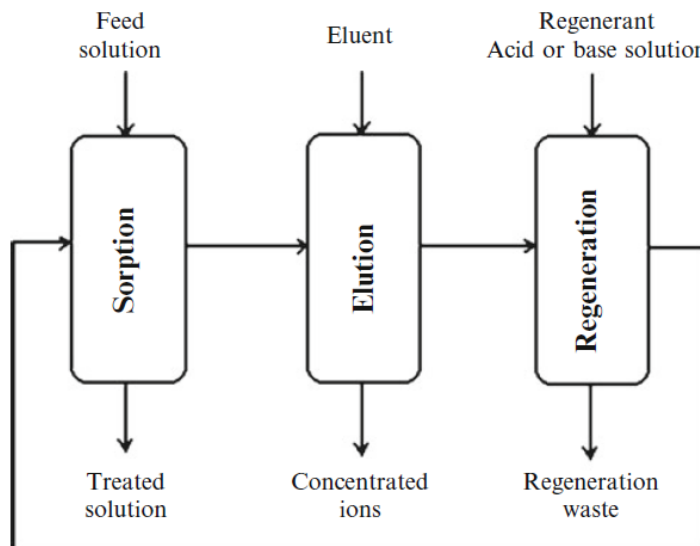


Figure 3-17 Schematic representation of ion exchange operation cycle

Most commonly, the ion exchange is performed in cyclic operations. Each cycle is divided into three main stages: (i) sorption, (ii) elution, and (iii) regeneration, as shown in the ion operation cycle schematized in Fig. (3.17). Details of ion operation cycle are as follows:

- i. Sorption: The solution containing the target ions is passed slowly through to reaction vessel. The ions bind into the resins. Ions initially contained in the exchanger are released.
- ii. Elution (stripping): The target ions are subsequently stripped from the loaded resin with a small volume of an eluent. The eluent replaces and hence also releases the target ions from the resin into the solution phase.
- iii. Regeneration: The principle of displacement of selectively binding ions by less selective binding ion is the basis for each regeneration procedure. Depending on the type of the ion exchanger and the stripping agent, most of the ion exchanger can be regenerated by acids (excess of  $H^+$  ions), salt-brines (excess of sodium or chloride ions), or alkali (excess of  $OH^-$  ions). During regeneration, the adsorbed ions are removed and replaced by suitable ions. For example, if the sorption step uses a cation exchanger loaded with  $H^+$  ions but the elution leaves  $Na^+$  ions in the exchanger phase, the material has to be protonated. A strong acid could be applied in order to convert (regenerate) the exchanger in the initial state. It is important to mention that designing an optimized cyclic ion exchange process requires efficient utilization of bed through selection of resins having high selectivity toward the target ions.

### 3.10. Advantages of Ion Exchange Processes

The widespread applications of ion exchange processes in various industrial aspects are supported by a combination of various advantages including the following:

- Proven ability to remove variety of impurities from various volumes with the availability of a wide number of resins.
- Tolerance for fluctuating feed flow rates.
- Low energy consumption.
- Accumulated experience that provides technically effective solutions that meet all system's design specifications.
- Large varieties of specific resins are available from suppliers. Each resin is effective in removing specific contaminants.
- Fast reaction and simple process operation.
- Can be operated at a high flow rate.
- The discharged effluents can achieve regulator acceptance.
- Cost-effectiveness which can be further improved by technical innovation including introducing cheap and highly tolerant ion exchange materials.
- The regenerant chemicals are cheap, and if well maintained, resin beds can last for many years before replacement is needed.

### 3.11. Limitations of Ion Exchange Process

Despite the extendable and diverse uses of the ion exchange process applications, there are a number of limitations which must be taken into consideration very carefully during the design stages. They include:

- High levels of suspended solids (greater than 10 ppm) and oil together with grease in wastewater may cause clogging of non-selective resins.
- Waste brine from regeneration step requires treatment and disposal, though waste volume can be reduced.
- Spent non-selective resins require frequent replacement and careful disposal.
- Competitive uptake by other ions may limit the effectiveness of non-selective exchange resins.
- Effectiveness of treatment is strongly influenced by water chemistry of the site(e.g., the presence of competing ions and pH of the water source).
- Oxidants present in the ground water may damage the ion exchange resin.
- Usually not feasible with high levels of total dissolved solids (TDS).
- Pre-treatment required for most surface water treatments.

### 3.12. Economy of Ion Exchange Processes

Ion exchange has long been proven to be a capable technology for removing many dissolved contaminants from various streams despite concerns over capital cost.

Capital and operational costs for ion exchange systems vary depending on a number of factors, such as the effluent discharge requirements, the volume of water to be treated, contaminant concentration, the presence of other contaminants, type of utilized resin and regenerant utilization, brine disposal, and site-specific hydrological and geochemical conditions. Among all, the key cost factors include

- (1) Pre-treatment requirements, (2) discharge requirements and resin utilization,
- (3) Regenerant used, and (4) efficiency.

The economy of the ion exchange process in an application can be optimized by:

- Selection of the right process based on the feed composition and the requirement of effluent to be discharged
- Selection of the type of ion exchange materials based on raw solution characteristics and optimum combinations of the operating parameters
- Selection of sorption and elution conditions taking into consideration that
  - (a) Sharper sorption front allows more efficiency in bed utilization
  - (b) Higher pumping rates allow higher productivity per unit time
  - (c) Higher concentration in the effluent causes more regeneration time
    - Optimization of regeneration including the type of regeneration agent and the degree of regeneration and the reuse of incompletely exhausted regenerating solution
    - Utilization of waste solution

The economy of the ion exchange processes can be further improved by process innovation. Particularly, introducing new ion exchange materials with low cost and high tolerance to feed concentrations are key issues in boosting cost reduction and expanding the usage of the technology to new frontiers. Also, introducing computer software and automation help very much to enhance the ion exchange process efficiency.

### 3.13. Applications of Ion Exchange Processes

The applications for ion exchange processes are numerous and cover wide range of industries and house appliances. The purpose of separation dictates the selection of the type of the ion

exchange materials, their physical form, and system configuration for practical application and thus forms the basis of a large number of ion exchange processes, which can be functionally divided into three main categories:

- Substitution: A valuable ion (e.g., copper and silver) can be recovered from solution and replaced by worthless one. Toxic ion such as cyanide can be similarly removed from solution and replaced by non-toxic one.
- Separation: A solution containing a number of different ions passes through a column containing beads of an ion exchange resin. The ions are separated and emerge following the order of their increasing affinity for the resin.
- Removal: By using combination of cation-exchange resin (in the  $H^+$  form) and an anion-exchange resin (in the  $OH^-$  form) or bipolar resins, all ions are removed and replaced by water ( $H^+OH^-$ ). The solution is thus demineralized.

Despite the diversity of ion exchange processes, their chief application of today is still the treatment of water with the principle offering of unlimited possibilities in other fields. Commercial ion exchange installations are serving in water and water treatment, food, and chemical industries include processes such as purification of sugar solutions, separation and purification of drugs and fine chemicals, purification of waste effluents, and the recovery of valuable wastes, for example, in the metallurgical industries, the extraction and quantitative separation of elements and metallic complexes.

## 3.14 Literature survey

### 3.14.1. Batch Technique:

Removal of hexavalent chromium from aqueous solutions by D301, D314 and D354 anion-exchange resins was studied by Taihong Shi et al. [28]. Batch shaking experiments were carried out to evaluate the adsorption capacity of resins (D301, D314 and D354) in the removal of chromium from aqueous solutions. Varying experimental conditions were studied, including  $\text{Cr}^{6+}$  concentrations, resin amounts, initial pH, contact time and temperatures. The ion-exchange process, which is pH-dependent, indicated the maximum removal of  $\text{Cr}^{6+}$  in the pH range of 1–5 for an initial concentration 100ppm of  $\text{Cr}^{6+}$ . It was found that more than 99.4% of the removal was achieved under optimal conditions. High adsorption rates of chromium for the three resins were observed at the onset, and then plateau values were gradually reached within 30 min. The experimental results obtained at various concentrations ( $27 \pm 1$  °C) showed that the adsorption pattern on the resins has followed Langmuir isotherms and the calculated maximum sorption capacities of D301, D314 and D354 were 152.52, 120.48 and 156.25 mg/g, respectively. The thermodynamic parameters (free energy change  $\Delta G^\circ$ , enthalpy change  $\Delta H^\circ$  and entropy change  $\Delta S^\circ$ ) for the sorption have been evaluated. It was also found that the adsorption of chromium on these anion-exchange resins follows first-order reversible kinetics.

Evaluation of Amberlite IRA96 and Dowex 1×8 ion-exchange resins for the removal of Cr(VI) from aqueous solution was studied by Serpil Edebalı et al [1]. Adsorption processes were carried out as a function of time, adsorbent dosage, pH and temperature to evaluate the performance of the resins. The optimum pH for Cr(VI) adsorption was found 3.0 for these resins. It was found that more than 93% removal was achieved under optimal conditions. The maximum adsorption capacities are 0.46 and 0.54 mmol/g of Amberlite IRA96 and Dowex 1×8 resin for Cr(VI) ion, respectively. The suitability of Freundlich and Langmuir adsorption models were investigated for Cr(VI)-resin equilibrium. A pseudo-second order kinetic model has been proposed to correlate the experimental data. The equilibrium adsorption level for Dowex 1×8 decreased with increasing temperature, while it increased for Amberlite IRA96.

The Removal of Cr(VI) from aqueous solution by two Lewatit-anion exchange resins was studied by Fethiye Gode et al. [6]. The sorption of hexavalent chromium, Cr(VI), from aqueous solutions on macroporous resins containing tertiary amine groups (Lewatit MP 62 and LewatitM610) was studied at varying Cr(VI) concentrations, adsorbent dose, pH, contact time and temperatures. The concentration of chromium in aqueous solution was determined by inductively coupled plasma spectrometry (ICP–AES). Batch shaking sorption experiments were carried out to evaluate the performance of LewatitMP62 and LewatitM610 anion exchange resins in the removal of Cr(VI) from aqueous solutions. The ion-exchange process, which is pH dependent, shows maximum removal of Cr(VI) in the pH range 2–6 for an initial Cr(VI) concentration of 100 ppm. The sorption increases with the decrease in pH and slightly decreases

with the increase in temperature. Both ion exchangers had high bonding constants with LewatitM610 showing stronger binding. It was observed that the maximum adsorption capacity of 0.40 mmol of Cr(VI)/g for Lewatit MP 62 and 0.41 mmol of Cr(VI)/g for Lewatit M 610 was achieved at pH of 5.0. The thermodynamic parameters (free energy change,  $\Delta G^\circ$ ; entropy change,  $\Delta S^\circ$ ; and, enthalpy change  $\Delta H^\circ$ ) for the sorption have been evaluated. The rise in temperature caused a slight decrease in the value of the equilibrium constant ( $K_c$ ) for the sorption of Cr(VI) ion. The sorption of Cr(VI) on the resin was rapid during the first 15 min and equilibrium was found to be attained within 30 min. The sorption of Cr(VI) onto the resins followed reversible first-order rate kinetics. Such ion exchange resins can be used for the efficient removal of chromium from water and wastewater.

Adsorptive removal of chromium (VI) from aqueous solutions and its kinetics study was studied by Souundarrajan M. et al. [29]. In their study, performance of chitosan coated carbon was evaluated for the removal of chromium (VI) from aqueous solution. Batch adsorption experiments were performed in order to examine the removal process under various factors like the effects of initial concentration, adsorbent dose, pH, and contact time. The metal ion removal was pH dependent and reached optimum at pH 5.0. Experimental data were analysed by Langmuir and Freundlich adsorption isotherms. The characteristic parameters and related correlation coefficients have been determined. The isotherm study revealed that the adsorption equilibrium is well-fitted to the Freundlich isotherm. Pseudo-first- and -second-order kinetic models were used for describing kinetic data. It was determined that removal of Cr (VI) was well-fitted by second-order reaction kinetic. The results showed that chitosan coated carbon are favorable adsorbent of Cr (VI) from aqueous solution.

Kinetics and equilibrium studies of adsorption of Cu(II) and Cr(VI) ions by chitosan was studied by Schmuhl R. et al. [30]. The ability of chitosan as an adsorbent for Cu (II) and Cr (VI) ions in aqueous solution was studied. The experiments were done as batch processes. Equilibrium studies were done on both cross-linked and non-cross-linked chitosan for both metals. Cr (VI) adsorption behaviour could be described using the Langmuir isotherm over the whole concentration range of 10 to 1000  $\text{mg}\cdot\text{l}^{-1}$  Cr. The maximum adsorption capacity for both types of chitosan was found to be 78  $\text{mg}\cdot\text{g}^{-1}$  for the non-cross-linked chitosan and 50  $\text{mg}\cdot\text{g}^{-1}$  for the cross-linked chitosan for the Cr (VI) removal. For the Cu (II) removal the Freundlich isotherm described the experimental data over the whole concentration range of 10 to 1000  $\text{mg}\cdot\text{l}^{-1}$  Cu (II). The maximum adsorption capacity for both types of chitosan can be estimated to be greater than 80  $\text{mg}\cdot\text{g}^{-1}$ . Cr (VI) removal was the highest at pH 5 but pH did not have a large influence on Cu (II). From these results it was clear that the adsorption of heavy metals is possible with chitosan, but that with this method, end concentrations of below 1  $\text{mg}\cdot\text{l}^{-1}$  can hardly be obtained.

Improved performance of a cellulose-based anion exchanger with tertiary amine functionality for the adsorption of chromium(VI) from aqueous solutions was studied by Anirudhan et al. [31]. A cellulose-based anion exchanger (Cell-AE) bearing  $-N^+H(CH_3)_2Cl^-$  functional groups was tested for its potential application in the removal of chromium(VI) from aqueous solutions. The Cell-AE was prepared through graft copolymerization of glycidylmethacrylate onto cellulose (Cell) in the presence of N,N -methylenebisacrylamide as a cross linker using benzoyl peroxide initiator, followed by amination and acidification. The adsorbent was characterized by infrared spectroscopy and X-ray diffraction studies. Batch experiments were performed to evaluate the adsorption efficiency of Cell-AE towards Cr(VI) ions. The contact time necessary to attain equilibrium and the optimum pH were found to be 1 h and 3.5, respectively. The adsorption process performed more than 99.4% of Cr(VI) removal from an initial concentration of 25.0mgL<sup>-1</sup>. The process followed a pseudo-second-order kinetics. Equilibrium data fitted very well with Sips isotherm. The maximum adsorption capacity of Cell-AE towards Cr(VI) was determined to be 126.87mgg<sup>-1</sup>. The electroplating industrial wastewater samples were treated with Cell-AE to demonstrate its efficiency in removing Cr(VI) from wastewater.

Adsorption mechanism of hexavalent chromium removal using Amberlite IRA 743 resin was studied by Muniyappan Rajiv Gandhi et al. [32]. A commercially available chelating resin namely, Amberlite IRA 743 (AMB) is a macroporous polystyrene Nmethylglucamine with free base form used for the removal of chromium from aqueous solution. AMB resin possesses an enhanced chromium sorption capacity (SC) of 20.41 mg/g in a minimum period of 30 min contact time. The sorption experiments were carried out in batch mode to optimize various influencing parameters viz., contact time, initial chromium concentration, pH, co-ions and temperature. The resin was characterized by FTIR and SEM with EDAX analysis. The mechanism of chromium removal by the resin was by means of electrostatic adsorption coupled reduction and complexation. The adsorption data was fitted with Freundlich and Langmuir isotherms. The calculated values of thermodynamic parameters namely  $\Delta G^\circ$ ,  $\Delta H^\circ$  and  $\Delta S^\circ$  indicated the nature of chromium sorption. The dynamic studies demonstrated that the sorption process follows pseudo-second-order and intraparticle diffusion models.

Adsorption thermodynamics and kinetics of Cr(VI) on KIP210 resin was studied by Jinbei Yang et al.[33]. Series of resin selection experiments were carried out and the KIP210 strong base anion exchange resin was confirmed to have the maximum equilibrium adsorption capacity to remove Cr(VI) from wastewater. The adsorption thermodynamics and kinetics of Cr(VI) on KIP210 resin were investigated completely and systematically. The static experiments were performed to study the effects of various parameters, such as shaking speed, resin dosage and pH during the adsorption process. The results indicated that the effect of external diffusion was eliminated at 160 rpm, the best pH value is 3.0 and the removal percentage of Cr(VI) increases with the increase of the resin dosage. The adsorption of Cr(VI) on KIP210 agrees well with the Langmuir isotherm and the adsorption parameters of thermodynamics are  $\Delta H = 26.5 \text{ kJ mol}^{-1}$ ,

$\Delta S = 126.7 \text{ J mol}^{-1} \text{ K}^{-1}$  and  $\Delta G < 0$ . It demonstrated that the adsorption of Cr(VI) on KIP210 is a spontaneously endothermic physisorption process. Moreover, the adsorption process can be described well by a pseudo-second-order kinetic model and the activation energy is  $30.9 \text{ kJ mol}^{-1}$ . The kinetic analysis showed that the adsorption rate is controlled by intraparticle diffusion. The resin was successfully regenerated using the NaOH solutions.

Sorption of Cr(VI) ions on two Lewatit-anion exchange resins and their quantitative determination using UV-visible spectrophotometer was studied by E. Pehlivan et al. [34]. The sorption of Cr(VI) from aqueous solutions with macroporous resins which contain quarternary amine groups (Lewatit MP 64 and Lewatit MP 500) was studied at varying Cr(VI) concentration, adsorbent dose, pH, contact time and temperature. Batch shaking sorption experiments were carried out to evaluate the performance of Lewatit MP 64 and Lewatit MP 500 anion exchange resins in the removal of Cr(VI) from aqueous solutions. The concentration of Cr(VI) in aqueous solution was determined by UV-visible spectrophotometer. The ion exchange process, which was dependent on pH, showed maximum removal of Cr(VI) in the pH range 3–7 for an initial Cr(VI) concentration of  $1 \times 10^{-3} \text{ M}$ . The optimum pH for Cr(VI) adsorption was found as 5.0 for Lewatit MP 64 and 6.0 for Lewatit MP 500. The maximum Cr(VI) adsorption at pH 5.0 was 0.40 and 0.41 mmol/g resin for Lewatit MP 64 and Lewatit MP 500 anion exchangers, respectively. The maximum chromium sorption occurred at approximately 60 min for Lewatit MP 64 and 75 min for Lewatit MP 500. The suitability of the Freundlich and Langmuir adsorption models was also investigated for each chromium-sorbent system. The uptake of Cr(VI) by the anion exchange resins was reversible and so it had good potential for the removal of Cr(VI) from aqueous solutions. Both ion exchangers had high bonding constants but Lewatit MP 500 showed stronger binding. The rise in the temperature caused a slight decrease in the value of the equilibrium constant ( $K_c$ ) for the sorption of Cr(VI) ion.

Equilibrium and kinetic studies of adsorption of toxic metal ion Cr(VI) from aqueous state by  $\text{TiO}_2$ -MCM-41: was studied by Kulamani Parida et al. [35]. Their paper dealt with the immobilization of various weight percentage of  $\text{TiO}_2$  on mesoporous MCM-41, characterization of the materials by X-ray diffraction (XRD), nitrogen adsorption-desorption, Fourier Transform Infrared (FTIR) analysis, UV-vis diffuse reflectance spectroscopy (DRS) and evaluation of the adsorption capacity toward Cr(VI) removal. It was found that the MCM-41 structure retained after loading of  $\text{TiO}_2$  but the surface area and pore diameter decreased due to pore blockage. Adsorption of Cr(VI) from aqueous state was investigated on  $\text{TiO}_2$ -MCM-41 by changing various parameters such as pH, metal ion concentration, and the temperature. When  $\text{TiO}_2$  loading was more than 20 wt.%, the adsorption activity (25) $\text{TiO}_2$ -MCM-41 reduced significantly due to considerable decrease in the surface area. It was also observed that  $\text{TiO}_2$  and neat MCM-41 exhibits very less Cr(VI) adsorption compared to  $\text{TiO}_2$ -MCM-41. The adsorption of Cr(VI) onto (20) $\text{TiO}_2$ -MCM-41 at pH  $\sim 5.5$  and temperature 323 K was 91% at 100 mg/L Cr(VI) metal ion concentration in 80 min. The experimental data fitted well to Langmuir and Freundlich

isotherms. The adsorption of Cr(VI) on TiO<sub>2</sub>-MCM-41 followed a second order kinetics with higher values of intra-particle diffusion rate. Thermodynamic parameters suggested that the adsorption process was endothermic in nature and desorption studies indicated a chemisorption mode.

Adsorption performance and mechanism of Cr(VI) using magnetic PS-EDTA resin from micro-polluted waters was studied by Ning Mao et al. [36]. Adsorption of Cr(VI) from aqueous solution onto a magnetic chelating resin with EDTA functionality (magnetic PS-EDTA) was investigated in a batch system. Various factors affecting the uptake behavior such as pH, contact time, initial concentration of the metal ions and dosage of resins on Cr(VI) removal were studied. The magnetic modified resin showed higher adsorption capacity and shorter adsorption equilibrium time for Cr(VI) compared with the raw PS-EDTA resin. The equilibrium data were analyzed using the Langmuir, Freundlich and Tempkin isotherm models among which Langmuir isotherm model was found to be suitable for the monolayer adsorption process. The monolayer adsorption capacity values of 123.05 mg/g for raw PS-EDTA and 250.00 mg/g for magnetic resin were very close to the maximum capacity values obtained at pH 4.0. Kinetic studies showed that the adsorption followed a pseudo second- order reaction. The mechanism was further identified by fitting intraparticle diffusion and McKay plots. The result indicated film diffusion was the rate-limiting step and intraparticle diffusion was also involved in adsorption. XPS spectra confirmed that reduction of Cr(VI) by Fe<sub>3</sub>O<sub>4</sub> nanoparticle on the resin occurred, while the electrostatic interaction between protonated amine groups and Cr(VI) anion played an important role in the adsorption. Furthermore, the resin could be regenerated through the desorption of the Cr(VI) anions using 0.5 M NaOH solution and could be reused to adsorb again.

Removal of chromium (VI) from synthetic wastewater using spectra/gel ion-exchange resin was studied by M. A. Barakat et al. [37]. Strong anion exchange resin (Spectra/Gel IE 1x8) has been investigated as adsorbent for the efficient removal of Cr(VI) ions from synthetic wastewater solutions. Batch experiments were conducted with initial Cr(VI) ions concentration ranging from 25-300 mg/L. Different parameters influencing Cr(VI) adsorption process such as; solution pH, Cr(VI) and adsorbent concentration and contact time were investigated. Results obtained revealed that Cr(VI) was successfully retained by the resin. Equilibrium was established within 30 minutes for initial Cr(VI) concentration up to 100 mg/L. The equilibrium data for adsorption of Cr(VI) was fitted with both Langmuir and Freundlich isotherms, however, Langmuir isotherm model was found to be more suitable for the Cr(VI) adsorption and maximum adsorption capacity of the Cr(VI) was found to be 173.8 mg/g. The adsorption process followed second order kinetics. The resin was regenerated by using 4M NaOH as an eluent with Cr(VI) adsorption efficiency higher than 83% after three regeneration cycles.

Effective adsorption of chromium (VI) from aqueous solutions using chitosan was studied by Agnieszka Adamczuk. [38]. In their work the adsorption process of chromium on chitosan flakes and powder was presented. The tests in the batch system were studied in equilibrium conditions in order to determine optimum parameters for loading chromium and were compared with those results reported in literature. The parameters investigated in this study included pH, contact time, initial concentration, sorbent dosage and temperature. The above described studies were also carried out for Cr(VI) adsorption in the presence of Cu(II), in order to compare the results with this competing ion. The experimental equilibrium parameters were obtained by fitting the experimental data by the Langmuir and Freundlich models. The process kinetics was evaluated by the pseudo first order, the pseudo second order and the intraparticle diffusion models. It was found that the pseudo second order kinetic model exhibited the highest correlation with the experimental data. Application of the Langmuir isotherm to the systems yielded the maximum sorption capacities of  $58.48 \text{ mg g}^{-1}$  and  $71.43 \text{ mg g}^{-1}$  for Cr(VI) and  $74.63 \text{ mg g}^{-1}$  and  $74.07 \text{ mg g}^{-1}$  Cr(VI) in the presence of Cu(II) onto chitosan powder and chitosan flakes, respectively. As followed from the thermodynamic parameters process is favourable, spontaneous and exothermic.

Batch study and kinetics of hexavalent chromium removal from aqueous solutions by anion exchange resin (Dowex 21 KCl) was studied by Hamdi Mihçioğur et al.[39]. In their study, the removal of hexavalent chromium (Cr), a strong oxidant and also carcinogen and mutagen, from aqua solution was done using ion exchange process. The batch experiments were conducted to study the kinetics of Cr removal for the concentrations of 1–20 mg/L Cr solutions. The ion exchange resin dosage was 1 g dry weight of ion exchanger/L for Dowex 21 KCl. The removal efficiency observed for all the Cr concentrations and mixing time was over the 82% for Dowex 21 KCl. During the batch experiments, four different mixing time (15–90 min) and six different pH values (2–7) were evaluated to determine the optimum mixing time and pH value. The highest removal efficiency of hexavalent Cr was obtained using 30 rpm shaker speed at pH 6. The experimental data fitted well to the pseudo-first- and pseudo-second-order kinetic models and then the rate constants were evaluated. Finally, it was concluded that the hexavalent chromium ion exchange kinetics of dowex 21 KCl was well explained by first order kinetic model rather than second order kinetic model.

Sorption of hexavalent chromium metal onto Amberlite IRA 410-equilibrium isotherms and kinetic studies was studied by Yasmine, AO.et al. [40]. The removal of chromium (VI) from aqueous solution by a strong anion exchanger Amberlite IRA 410 was studied. Batch mode experiments were conducted to study the effect of the initial concentration of Cr (VI) and the equilibrium isotherms. The sorption process of chromium (VI) was tested with Freundlich, Langmuir and Khan Models, and the results showed that sorption behaviour of chromium (VI) followed a Langmuir isotherm, namely a monolayer sorption onto the resin surface. The sorption capacity was determined to be  $153.8 \text{ mg/g}$ . Elovich, Ritchie and the pseudo-second order models were tested to represent kinetic data and the equation parameter values were evaluated. It was found that the sorption kinetics followed a pseudo-second order model in the concentration range 0-100 mg/l, while above 100 mg/l the Ritchie model matched experimental kinetic data. In

addition, the capacity of sorption increased for increasing initial Cr(VI) concentration. The thermodynamic parameters for the sorption process have been evaluated. The entropy change  $\Delta S$  was found to be 318.4 J/K/mol, the heat of adsorption (enthalpy change)  $\Delta H$  was 85.2 kJ/mol indicating the endothermic nature of the adsorption process, and a decrease of the Gibbs free energy ( $\Delta G$ ) for increasing temperatures indicated the spontaneous nature of the process.

Adsorption of Aqueous Cr(VI) by Novel Fibrous Adsorbent with Amino and Quaternary Ammonium Groups was studied by J.Wang et al. [41]. A novel fibrous adsorbent functionalized with both amino and quaternary ammonium groups (QAPAN) was prepared through a simple two-step route (i.e., amination followed by quaternization reactions) for removing aqueous Cr(VI) through batch and column experiments. As compared with traditional adsorbents, the QAPAN had an extremely fast adsorption kinetic (equilibrium achieved within 10 min) and an exceptionally high adsorption capacity ( $Q(m) = 248$  mg/g). The QAPAN worked well even in strong basic conditions, and ionic strength and coexisting anions had minor inhibitory effects on the adsorption. Besides, the QAPAN could be repeatedly used for Cr(VI) adsorption with no obvious decrease of uptake after regeneration with 0.1 mol/L NaOH. By analyzing FTIR and XPS spectra, an electrostatic interaction mechanism between Cr(VI) oxyanions and the surface amino and quaternary ammonium groups was proposed. Findings of the current study provided a novel material and technology for treatment of Cr(VI) contaminated waters.

Adsorption and desorption properties of D318 resin for Cr(VI) was studied by SHU Zeng-nian et al. [42]. Experimental results showed that D318 resin has the best adsorption ability for Cr(VI) at pH=3.16 in HAc-NaAc medium. The statically saturated adsorption capacity of the resin is 265.4 mg/g. The thermodynamic adsorption parameters, enthalpy change  $\Delta H$  and free energy change  $\Delta G_{298}$  of the adsorption reaction are 4.81 and  $-5.16$  kJ/mol, respectively. The apparent activation energy  $E_a$  is 22.4 kJ/mol. The adsorption behavior obeys the Freundlich isotherm. The molar coordination ratio of the functional group of resin to Cr(VI) was 3:2. Cr(VI) adsorbed on D318 resin can be eluted by 5%NaOH-5%NaCl quantitatively.

Removal of chromium from electroplating industry effluents by ion exchange resins was studied by Sofia et al. [43]. The main objective of the present work is to evaluate the performance of commercial ion exchange resins for removing chromium trivalent from industrial effluents, and for this purpose two resins were tested: a chelating exchange resin (Diaion CR11) and a weak cationic resin (Amberlite IRC86). In order to evaluate the sorption capacity of the resins some equilibrium experiments were carried out, being the temperature and pH the main variables considered. The chromium solutions employed in the experiments were synthetic solutions and industrial effluents. In addition, a transient test was also performed as an attempt to understand the kinetic behaviour of the process.

Batch kinetics and thermodynamics of chromium ions removal from waste solutions using synthetic adsorbents was studied by Gasser M.S et al. [44].  $Mg(OH)_2$  was identified as a

component in the magnesia cement being adsorbent for Cr(VI). Modified magnesia cement was prepared by the addition of ferric chloride and humic acid. The equilibrium adsorption of Cr(VI) on magnesia cement adsorbents (MF5-1) and (MF5-2) was investigated as a function of contact time, adsorbent weight, solute concentration and temperature. Tests of different isotherms have shown that the adsorption data fit the Langmuir and Freundlich isotherms at  $25 \pm 1$  °C. The nature of the diffusion process responsible for adsorption of Cr(VI) on (MF5-1) and (MF5-2) adsorbents was discussed. The kinetics and mechanism of diffusion of Cr(VI) into (MF5-1) and (MF5-2) adsorbents from aqueous solution have been studied as a function of Cr(VI) concentrations and reaction temperatures. The adsorption of Cr(VI) on the MF5-1 and MF5-2 adsorbents followed first-order reversible kinetics. The forward and backward constants,  $k_1$  and  $k_2$  have been calculated at different temperatures between 10 and 50 °C. The heat of activation of the adsorption,  $\Delta H^*$  and  $\Delta S^*$  were calculated for Cr(VI) at 25 °C. The values of  $\Delta H^*$  were found 18.1 and 10.7 kJ mol<sup>-1</sup> for MF5-1 and MF5-2, respectively, while entropy change,  $\Delta S^*$ , were found -106.8 and -118.6 J mol<sup>-1</sup> K<sup>-1</sup> for MF5-1 and MF5-2, respectively. The study showed that pore diffusion is the rate-determining step in the adsorption of Cr(VI) ions for MF5-1 and MF5-2. MF5-2 was found more efficient for Cr(VI) adsorption than MF5-1. Also Cr(VI) can be adsorbed on MF5-2, whereas Cr(III) cannot. So, the competitive adsorption of multi-metals onto the MF5-2 adsorbent was studied. The studies showed that this adsorbent can be used as an efficient adsorbent material for the removal of Cr(VI) from water and nuclear power plant coolant water.

Kinetics of removal of chromium from water and electronic process wastewater by ion exchange resins: 1200H, 1500H and IRN97H was studied by S. Rengaraj et al. [45]. Ion exchange resins 1200H, 1500H and IRN97H showed a remarkable increase in sorption capacity for chromium, compared to other adsorbents. The adsorption process, which was pH dependent show maximum removal of chromium in the pH range 2–6 for an initial chromium concentration of 10 mg/l. The metal ion adsorption obeyed linear, Langmuir and Freundlich isotherms. The adsorption of chromium on these cation exchange resins followed first-order reversible kinetics and pseudo-first-order kinetics. The intraparticle diffusion of chromium on ion exchange resins represented the rate-limiting step. The uptake of chromium by the ion exchange resins was reversible and thus have good potential for the removal/recovery of chromium from aqueous solutions. They conclude that such ion exchange resins can be used for the efficient removal of chromium from water and wastewater.

Removal of hazardous hexavalent chromium from aqueous solution using divinylbenzene copolymer resin was studied by S. Bajpai et al. [46]. Their paper presented the removal of hazardous hexavalent chromium from liquid waste streams using divinylbenzene copolymer resin Amberlite IRA 96. Important sorption parameters such as contact time, pH, resin dosage and initial metal concentration were studied at 30 °C . The kinetic study was conducted using pseudo-first and pseudo-second-order kinetics at 30 °C. The sorption process was found to be pH

dependent. Maximum removal was obtained at pH 2 under optimized conditions. The sorption process was rapid and 99 % of the removal was achieved in first 30 min. The equilibrium data were fitted to both Langmuir and Freundlich models. The better regression coefficient ( $R^2$ ) in Freundlich model suggested the multilayer sorption process. The value of Gibbs free energy for sorption process was found to be  $-12.394 \text{ kJmol}^{-1}$ . The negative value indicated the spontaneity of the sorption process. Scanning electron microscope and energy dispersive X-ray spectroscopy studies were conducted to find the role of surface morphology during sorption process. The Fourier transform infrared study was conducted to identify the functional groups responsible for interaction between the resin and chromium. Desorption and regeneration studies were also carried out.

Mechanisms of Cr(VI) removal from synthetic wastewater by low cost adsorbents was studied by Manjeet Bansal et al. [47]. In their study the removal of Cr(VI) from aqueous solutions by batch adsorption technique using different low cost adsorbents was investigated. Adsorbents such as rice husk a surplus agricultural byproduct, saw dust a timber industry waste were used to determine adsorption efficiency. The influence of pH, adsorbent dose, initial Cr(VI) concentration and contact time on the selectivity and sensitivity of the removal process was investigated. Adsorption process was found to be highly pH dependent. Optimum pH for adsorption of Cr(VI) was found to be 2.0. Kinetic studies were performed to understand the mechanistic steps of the adsorption process and rate kinetics for the adsorption of Cr(VI) was best fitted with pseudo -second order kinetic model. EDAX of the Rice husk and Sawdust (native and metal loaded) were recorded to explore the elemental constitution of the adsorbents. Reusability of the adsorbents was examined by desorption in which HCl eluted 84.08% and 79.63% Cr(VI) from Rice husk and Sawdust, respectively. Langmuir and Freundlich isotherms were applied to the adsorption process and their constants were evaluated. The adsorption capacity  $q_{\text{max}}$  calculated from Langmuir isotherm obtained for the different adsorbents showed that sawdust was the most effective among the selected adsorbents for the removal of Cr(VI) from aqueous solutions.

Removal of chromium (VI) from aqueous solutions using Lewatit FO36 nano ion exchange resin was studied by Rafati, L et al. [48]. The removal of the chromium (VI) ion from aqueous solutions with the Lewatit FO36 ion-exchange resin was described at different conditions. The effects of adsorbent dose, initial metal concentration, contact time and pH on the removal of chromium (VI) were investigated. The batch ion exchange process was relatively fast and it reached equilibrium after about 90 min of contact. The ion exchange process, which was pH dependent showed maximum removal of chromium (VI) in the pH range 5.0-8.0 for an initial chromium (VI) concentration of  $0.5 \text{ mg/dm}^3$ . The equilibrium related to Lewatit FO36 ion-exchange capacity and the amounts of the ion exchange were obtained using the plots of the Langmuir adsorption isotherm. It was observed that the maximum ion exchange capacity of 0.29

mmol of chromium (VI)/g for Lewatit FO36 was achieved at optimum pH value of 6.0. The ion exchange of chromium (VI) on this cation exchange resin followed first-order reversible kinetics.

Removal of hexavalent chromium by new quaternized crosslinked poly(4-vinylpyridines) was studied by Violeta Neagu et al. [49]. New quaternized crosslinked poly(4-vinylpyridines) prepared by nucleophilic substitution reactions of 4-vinylpyridine: divinylbenzene copolymers of gel and porous structure with halogenated compounds such as benzyl chloride and 2-chloroacetone, were used to remove Cr(VI) from the aqueous solution. Batch adsorption studies were carried out to determine the effect of the initial concentration of Cr(VI), pH, temperature and the presence of sulfate anions. The process was found to be pH and concentration dependent. The adsorption capacities increased with the increase of the initial concentration of Cr(VI) and both resins exhibited the degrees of usage of the exchange capacities higher than 90% and good efficiency in the chromium removal. Equilibrium modeling of the process of Cr(VI) removal was carried out by using the Langmuir and Freundlich isotherms. The experimental data obeyed these isotherm models. The thermodynamic parameters (free energy change  $\Delta G$ , enthalpy change  $\Delta S$  and entropy change  $\Delta H$ ) for the adsorption have been evaluated and therefore, it was showed the spontaneous and endothermic process of the adsorption of Cr(VI) on the pyridine resins. In the competitive adsorption studies, chromate/ sulfate revealed the selectivity of the pyridine adsorbents towards chromium ions. At acidic pH the synthesized pyridine resins offered much greater chromate removal capacities compared to alkaline pH. In the competitive adsorption studies, chromate/sulfate revealed the selectivity of the pyridine adsorbents towards chromium ions due to the formation a sandwich arrangement with the chromium anion and functional groups attached to the quaternary nitrogen atom.

Adsorption of Cr(VI) using synthetic poly(m-phenylenediamine) was studied by Wanting Yu et al.[50]. Poly(m-phenylenediamine) (PmPD) with different oxidation state was successfully synthesized by the improved chemically oxidative polymerization. The function of oxidation state on Cr(VI) adsorption was systematically examined through adsorption experiments. Results showed that the Cr(VI) adsorptivity of all PmPD increased with decreasing the initial pH. When the oxidation state of PmPD was dropped, the equilibrium time for Cr(VI) adsorption was obviously shortened and its Cr(VI) removal and adsorption selectivity were profoundly obviously increased. Typically, PmPD with the lowest oxidation state in this research possesses the highest Cr(VI) removal of 500 mg g<sup>-1</sup>. Moreover, PmPD with lower oxidation state displays a potentially superior prospect in Cr(VI) treatment through preliminary experiments on 5 cycles of adsorption, column adsorption and practical wastewater treatment. The possible adsorption mechanism was discussed mainly according to characterizations (FTIR, XPS) and experiments, which together suggested that the Cr(VI) adsorption most possibly involve redox reaction, chelation and doping adsorption.

Study on chromium(VI) ion sorption on anion-exchange resin Amberlite IRA 910 was studied by Wojcik, G. et al.[51]. Cr(VI)-containing ions were removed from their aqueous solutions. (pH 1.5-7, initial concentration up to 2000 ppm) by sorption on a macroporous strongly basic anion-exchange resin for 360 min. The sorption kinetics was described by 1st and 2nd order equations, the sorption equilibrium by Langmuir and Freundlich isotherm equations. A partial reduction of sorbed Cr(VI) to Cr(III) was observed.

Synthesis and Characterization of a Few Amino-Functionalized Copolymeric Resins and Their Environmental Applications was studied by Gandhi MR. et al.[52]. The synthetic copolymeric resins acrylonitrile/divinylbenzene/vinylbenzylchloride (AN/DVB/VBC), styrene/divinylbenzene/vinylbenzyl chloride (ST/DVB/VBC), and vinylbenzyl chloride/divinylbenzene (VBC/DVB) have been prepared by suspension polymerization. These polymeric matrixes were aminated with ethylenediamine (ED) and then protonated to increase their selectivity toward Cr(VI). The experiments were carried out in batch mode to optimize various influencing parameters, namely, contact time, pH, other interfering co-ions, and temperature. The chromium removal capacity (CRC) of AN/DVB/VBC ED resin was found to be higher than those of the other prepared copolymers. The mechanism of chromium removal was governed by electrostatic-adsorption-coupled reduction and complexation. The polymeric resins and chromium-sorbed resins were characterized by FTIR, SEM-EDAX, BET, elemental analysis, and EPR studies. The adsorption data were fitted with Freundlich and Langmuir isotherms. The calculated values of thermodynamic parameters indicated the nature of chromium sorption.

Synthesis of N-Methylimidazolium Functionalized Strongly Basic Anion Exchange Resins for Adsorption of Cr(VI) was studied by Lili Zhu et al.[53]. N-Methylimidazolium functionalized strongly basic anion exchange resins in the Cl<sup>-</sup> form (RCI) and SO<sub>4</sub><sup>2-</sup> form (R(2)SO(4)) were synthesized and employed for adsorption of Cr(VI) from aqueous solution. FT-IR and elementary analysis proved the structures of anion exchange resins and the content of functional groups. The gel-type strongly basic anion exchange resins had high thermal stability according to TGA and good chemical stability under the experimental conditions. The adsorption behaviors of Cr(VI) on RCI and R(2)SO(4) were studied using the batch technique. It was shown that adsorption equilibrium was reached rapidly within 60 min. The adsorption data for RCI and R(2)SO(4) were consistent with the Langmuir isotherm equation. The maximum adsorption capacities of RCI and R(2)SO(4) were 132 and 125 mg/g, respectively, with almost all active sites fully occupied. RCI and R(2)SO(4) could be used in the wide pH range 1-12 and were very suitable to remove Cr(VI) at a low concentration level. They also showed great preference to Cr(VI) compared to the other counterions. RCI was easily regenerated using the mixed solution of 0.3 mol/L NaOH and 0.3 mol/L NaCl, and retained nearly 100% of its original capacity during four cycles.

Continuous electrodeionization for removal and recovery of Cr(VI) from wastewater was studied by YQ Xing et al.[54]. Continuous electrodeionization (CEDI) was investigated for removal and recovery of Cr(VI) from synthetic wastewater. Different anion exchange resins, including the gel strong-base resin, gel weak-base resin, macro-porous strong-base resin, and macro-porous weak-base resin, were examined. The gel strong-base resin was found to be the best one for use in

CEDI. It was shown that CEDI could remove and recover Cr(VI) effectively from wastewater. After treatment, Cr(VI) concentration was reduced from initial 40-100 mg/L to 0.09-0.49 mg/L, and a pure chromic acid solution containing Cr(VI) as high as 6300 mg/L Cr(VI) was obtained. The current efficiency and energy consumption was 16.1-18.8%, and 4.1-7.3 kWh/mol Cr(VI), respectively.

Removal of Cr(VI) and As(V) ions from aqueous solutions by polyacrylate and polystyrene anion exchange resins was studied by Jachula Justyna et al.[55]. The sorption of Cr(VI) and As(V) from the aqueous solutions with the polyacrylate anion exchangers of the strong base functional groups Amberlite IRA 458 and Amberlite IRA 958 was studied. The studies were carried out by the static-batch method. The concentration of Cr(VI) and As(V) ions in the aqueous solution was determined by the UV-VIS spectrophotometer. The influence of several parameters was studied with respect to sorption equilibrium. The phase contact time and the concentration affected the sorption process. The equilibrium state was established already after 15 min of phase contact time. Maximum uptake of Cr(VI) and As(V) occurred at pH 5 and 10, respectively. The determined kinetic parameters implied that the sorption process proceeds according to the equation type of pseudo second-order. Sorption equilibrium data were correlated with the Langmuir and Freundlich isotherms. Removal of As(V) ions on macroporous Amberlite IRA 900 decreased about 12 % in presence of other anions ( $\text{Cl}^-$ ,  $\text{NO}_3^-$ ,  $\text{SO}_4^{2-}$ ) in the solution. The sorption was temperature dependent

Kinetics, thermodynamic, and adsorption studies on removal of chromium(VI) using Tulsion A-27(MP) resin was studied by Koujalagi, PS. Et al.[56]. The kinetics, thermodynamic, and adsorption studies on removal of chromium(VI) from aqueous and in presence of industrial solvents 2-methoxyethanol and 2-ethoxyethanol with macroporous resin Tulsion A-27 was studied at varying concentration of Cr(VI), adsorbent dosage, pH, contact time, and temperature. Batch shaking sorption experiments were carried out to evaluate the performance of Tulsion A-27(MP) anion exchange resin in the removal of Cr(VI) from aqueous and mixed aqueous solvents, 2-methoxyethanol and 2-ethoxyethanol. The concentrations of Cr(VI) in aqueous and mixed aqueous solvents were determined by UV-Visible spectrophotometer. As the adsorption process was pH dependent, it showed maximum removal efficiency of Cr(VI) in the pH range of 5-6 for an initial chromium concentration of 0.0011 M. Effect of temperature on the equilibrium constant was studied and the thermodynamic parameters were evaluated. Kinetic experiments revealed the dominance of adsorption. The sorption models, Langmuir and Freundlich adsorption isotherms, were discussed on amount of Cr(VI) uptake. The resin was analyzed by infrared spectroscopy and scanning electron microscopy before and after the adsorption process. The sorption of Cr(VI) by the anion exchange resin was reversible and so it has good potential for the removal/recovery of Cr(VI) from aqueous and mixed aqueous solvents. The anion exchange resin can be used for the efficient removal of Cr(VI) from water and wastewater.

Batch sorption dynamics, kinetics and equilibrium studies of Cr(VI), Ni(II) and Cu(II) from aqueous phase using agricultural residues was studied by Rajvinder Kaur et al.[57]. In their study, the agricultural residues viz., *Syzygium cumini* and *Populus deltoides* leaves powder have been used for the biosorption of Cu(II), Ni(II), and Cr(VI) from aqueous solutions. FTIR and

SEM analysis of the biosorbents were performed to explore the type of functional groups available for metal binding and to study the surface morphology. Various physico-chemical parameters such as pH, adsorbent dosage, initial metal ion concentration, and equilibrium contact time were studied. Thermodynamic studies were carried out and the results demonstrated the spontaneous and endothermic nature of the biosorption process. The equilibrium data were tested using four isotherm models—Langmuir, Freundlich, Temkin and Dubinin–Radushkevich and the maximum biosorption capacities were evaluated. The Pseudo-first-order, pseudo-second-order, Elovich and intraparticle diffusion models were applied to study the reaction kinetics with pseudo-second order model giving the best fit ( $R^2 = 0.99$ ) to the experimental data.

Optimization and Modeling of Hexavalent Chromium Removal From Aqueous Solution Via Adsorption on Multiwalled Carbon Nanotubes was studied by Mina Gholipour et al.[58]. In their article, removal of hexavalent chromium via adsorption on multiwalled carbon nanotubes was investigated as a function of adsorbent dosage, initial solution pH, initial Cr(VI) concentrations, contact time and temperature. The batch experiments were conducted at 3 different temperatures (17, 27 and 37°C) and shows that Cr(VI) removal obeys pseudo-second order rate equation. Rate constant (K) values in 3 temperatures, pre-exponential factor and adsorption activation energy (E) was also obtained. The sorption data fitted well with Freundlich isotherm adsorption model. Thermodynamic parameters such as Gibbs free energy ( $\Delta G^\circ$ ), enthalpy ( $\Delta H^\circ$ ) and entropy ( $\Delta S^\circ$ ) for Cr(VI) adsorption were estimated and Results suggest that the adsorption process is a spontaneous and endothermic.

Equilibrium and kinetics of heavy metal ion exchange was studied by Hsien Lee et al.[59]. A series of ion-exchange equilibrium tests of  $\text{Cu}^{2+}/\text{H}^+$ ,  $\text{Zn}^{2+}/\text{H}^+$ , and  $\text{Cd}^{2+}/\text{H}^+$  systems using Amberlite IR-120 were performed. The equilibrium data were analysed by the Langmuir isotherm, Freundlich isotherm, and selectivity coefficient approaches. The thermodynamic parameters such as Gibbs free energy change, enthalpy change, and entropy change were calculated. By comparison of the selectivity coefficients, the affinity sequence to IR-120 is  $\text{Cu}^{2+} > \text{Zn}^{2+} > \text{Cd}^{2+} > \text{H}^+$ . Moreover, in order to understand the heavy metal extraction kinetics in the presence of Amberlite IR-120, the ion exchange kinetics was also studied. The ion-exchange kinetic data were regressed by the pseudo first-order, second-order models, and a reversible reaction model. The activation energies calculated from the rate coefficients at different temperatures are 15.41, 7.04, and 17.01 kJ/mol for copper, zinc, and cadmium, respectively. Although the pseudo first- and second-order models were easier to use for data analysis, the resultant model parameters depend on operating conditions. The reversible reaction model was capable to predict the effects of resin to solution ratio, initial heavy metal concentration, and temperature on the ion-exchange kinetic curves

Integration of ion exchange and electrodeionization as a new approach for the continuous treatment of hexavalent chromium wastewater was studied by Lucía Alvarado et al.[60]. In their work, continuous ion exchange and electrodeionization are proposed as a new hybrid technology for the effective treatment of Cr(VI) wastewater as well as the recovery of chromium ions. They have systemically studied a strong basic macroreticular anion exchange resin (AmberliteIRA900) for the removal of Cr(VI). The ion exchange isotherm and kinetics of the resin were determined, showing that the IRA900 anionic ion exchange resin has a high capacity for ion exchange with hexavalent chromium (116 mg Cr(VI) per gram of resin). When the anionic resin was combined with a strong acidic macroreticular cation exchange resin (Amberlite 200C) and employed in continuous electrodeionization, over 98.5% of Cr(VI) was continuously removed from the dilute compartment with an energy consumption of less than 0.07 kW h/m<sup>3</sup>, while Cr(VI) was recovered in the concentrate compartment.

Hexavalent chromium removal mechanism using conducting polymers was studied by K.K. Krishnani et al.[61]. Their paper reported detoxification of Cr(VI) into Cr(III) using electrochemically synthesized polyaniline (PANI), polypyrrole (PPY), PANI nanowires (PANI-NW) and palladium-decorated PANI (PANI-Pd) thin films. Percent Cr(VI) reduction was found to be decreased with an increase in pH from 1.8 to 6.8 and with initial Cr(VI) concentration ranging from 2.5 to 10 mg/L. Efficacy of PANI increased at higher temp of 37 °C as compared to 30 °C. PANI-Pd was found to be most effective for all three initial Cr(VI) concentrations at pH 1.8. However, efficacy of PANI-Pd was significantly reduced at higher pHs of 5 and 6.8. Efficacy of PANI and PANI-NW was found to be nearly the same. However, there was a significant reduction in effectiveness of PANI-NW at 10 mg/L of Cr(VI) at all the three pHs studied, which could be attributed to degradation of PANI-NW by higher initial Cr(VI) concentration. PPY and PANI-NW were found to be highly sensitive with respect to pH and Cr(VI) initial concentration. Chromium speciation on PANI film was carried out by total chromium analysis and XPS, which revealed Cr(III) formation and its subsequent adsorption on the polymer. PANI-Pd and PANI were recommended for future sensor applications for chromium detection at low pH.

Adsorptive Removal of Chromium (VI) from Aqueous Solution Using Cow Hooves was studied by Ilesanmi Osasona et al.[62]. The adsorption process, which was carried out through batch method, was investigated over a range of pH (2-7), agitation time (0-150 mins.) and adsorbent mass (1.0-3.0 g per 50 mL of metal solution). The adsorption isotherms were obtained using initial metal concentrations ranging from 15 to 100 mgL<sup>-1</sup>. After agitation, the resultant solution was analyzed for Cr (VI) using Atomic Absorption Spectrophotometer. The optimum operating parameters obtained for the adsorption process are pH 2 (89.5% removal) and time of 30 mins (34.4% removal) while the highest metal uptake (mgg<sup>-1</sup>) was recorded for 1g of the adsorbent per 50ml of solution. Langmuir, Freundlich and Dubinin-Raduskevich (D-R) isotherm models were applied to describe the experimental data. The Langmuir maximum adsorption capacities of the cow hoof for Cr (VI) at 298, 308 and 318 K were determined to be 3.57, 4.81 and 5.71 mgg<sup>-1</sup>

respectively. Freundlich isotherm model fitted the equilibrium data better than Langmuir and D-R models. The mean free energy ( $E$ ) which was calculated from D-R model indicated that the sorption process was dominated by physisorption mechanism. The adsorption kinetics was found to follow the pseudo-second-order model.

Chromium (VI) removal from aqueous solutions by purolite base anion--exchange resins with gel structure was studied by Catalin Balan et al; [63]. The removal of Cr (VI) from aqueous solution using two strong base anionic resins with gel structure, purolite A-400 (styrene-divinylbenzene matrix) and purolite A-850 (acrylic matrix) was investigated using a batch technique. The sorption efficiency was determined as a function of phases contact time, solution pH, resin dose, temperature and initial Cr (VI) concentration. The percentage of Cr (VI) removed reached maximum values (up to 99%) in the pH range 4.0–5.3 at a resin dose of 6 g/L and Cr (VI) concentration up to 100 mg/L. An increase in temperature had a positive effect on the Cr (VI) sorption process. The equilibrium sorption data were fitted with the Freundlich, Langmuir and Dubinin-Radushkevich isotherm models, using both linear and nonlinear regression methods. The Langmuir model verified the experimental data very well and gave a maximum sorption capacity of 120.55 and 95.82 mg Cr (VI)/g for the A-400 and A-850 resins, respectively. The thermodynamic study and mean free energy of sorption values calculated using Dubinin-Radushkevich equation indicated the sorption is a chemical endothermic process. The kinetic data were well described by the pseudo-second order kinetic equation and the sorption process is controlled by external (film) diffusion and intraparticle diffusion.

Equilibrium and kinetic studies of Copper and chromium(VI) removal by chitosan derivatives was studied by George Z. Kyzas et al; [64]. Chitosan sorbents, cross-linked and grafted with amido or carboxyl groups, were prepared and their sorption properties for Cu(II) and Cr(VI) uptake were studied. Equilibrium sorption experiments were carried out at different pH values and initial ion concentrations. The equilibrium data were successfully fitted to the Langmuir–Freundlich (L–F) isotherm. The calculated maximum sorption capacity of the carboxyl grafted sorbent for Cu(II) was found to be 318 mg/g at pH 6, while the respective capacity for Cr(VI) uptake onto the amido-grafted sorbent was found to be 935 mg/g at pH 4. Thermodynamic parameters of the sorption process such as  $\Delta G^0$ ,  $\Delta H^0$ , and  $\Delta S^0$  were also calculated. The experimental kinetic data were successfully fitted to a novel phenomenological diffusion-reaction model (DIFRE), which combines: (i) mass transfer of the metal ions from the bulk solution on the sorbent surface; (ii) diffusion of the ions through the swollen polymer particle; and (iii) instantaneous local chelation (for cations) or electrostatic attraction (for anions) on the amino groups of the polymer. The regeneration of sorbents was affirmed in four sequential cycles of sorption–desorption experiments, without significant loss in sorption capacity.

Biosorption characteristics of  $\text{Cr}^{6+}$  from aqueous solutions by *pinus sylvestris* l. timber fillings was studied by Ackmez Mudhoo et al; [65]. *Pinus Sylvestris* L. timber fillings were boiled and utilized as a biosorbent for the removal of  $\text{Cr}^{6+}$  from a synthetic wastewater. The  $\text{Cr}^{6+}$  removal increased from 34.8% to 69.41% as biosorbent dosage increased from 3.0 to 8.0 g/L, while the uptake of  $\text{Cr}^{6+}$  decreased from 6.09 mg/g to 4.78 mg/g as the biosorbent dosage increased from 3.0 to 8.0 g/L, when the initial  $\text{Cr}^{6+}$  concentration was 50 mg/L. The experimental equilibrium data were well described by both the Langmuir and Dubinin-Radushkevich adsorption isotherm models. Based on  $R^2$  values, the Langmuir model fitted the equilibrium biosorption data best, confirming monolayer adsorption of  $\text{Cr}^{6+}$  onto the biosorbent surface. The biosorption kinetics of  $\text{Cr}^{6+}$  was best described by pseudo-second-order kinetics since at all concentrations; the  $R^2$  values were higher than the corresponding pseudo-first order values. The overall results indicated that *P. Sylvestris* L. is a promising biosorbent for  $\text{Cr}^{6+}$  removal from dilute aqueous solutions.

Kinetic and thermodynamic studies of chromium (VI) sorption by pure and carbonized fluted pumpkin waste biomass (*Telfairia occidentalis* Hook F.) was studied by Timi Tarawou et al; [66]. The adsorption of chromium (VI) ions from aqueous solution was studied using pure and carbonized fluted pumpkin waste biomass (FPWB). The kinetic data shows a pseudo-first-order mechanism with rate constants of  $1.26 \times 10^{-2}$  and  $1.933 \times 10^{-2} \text{ mg g}^{-1} \text{ min}^{-1}$  for the pure and carbonized FPWB, respectively. While the pseudo-second-order mechanism has rate constants of  $0.93 \times 10^{-1}$  and  $1.33 \times 10^{-1} \text{ mg g}^{-1} \text{ min}^{-1}$  for the pure and carbonized waste biomass respectively. The pseudo-second order kinetic model was found to be more suitable for describing the experimental data based on the correlation coefficient values ( $R^2$ ) of 0.9975 and 0.9994 obtained for pure waste biomass (PWB) and carbonized waste biomass (CWB), respectively. The results obtained from this study show that PWB and CWB have very high removal capacity for chromium (VI) from aqueous solution over a range of reaction conditions. Thus, fluted pumpkin waste biomass (*Telfairia occidentalis* Hook F) is a potential sorbent for the treatment of industrial effluents containing chromium (VI) contaminant.

Studies on removal of Cr(VI) and Cu(II) ions using Chitosan-grafted- polyacrylonitrile was studied by A. Shanmugapriya et al; [67]. In their work, graft copolymerization of polyacrylonitrile onto chitosan has been carried out in the presence of ceric ammonium nitrate redox initiator. Chitosan has been used as an adsorbent for the removal of heavy metal ions from aqueous solution through adsorption process. The property of chitosan is enhanced by grafting. The prepared copolymer was characterized by FTIR, XRD and SEM. The effect of pH, contact time and amount of adsorbent dose were also investigated. The adsorption kinetics of chitosan-g-polyacrylonitrile was found to follow pseudo-second-order kinetic model. The experimental data were fitted to Langmuir adsorption isotherms.

### 3.14.2.Fixed Bed Column:

Adsorption of hexavalent chromium from aqueous solution by modified corn stalk: A fixed-bed column study was studied by Suhong Chen et al. [3]. Continuous fixed-bed column studies were carried out by using modified corn stalk (MCS) as an adsorbent for the removal of Cr(VI) from aqueous solution. The effect of various parameters like bed depths (1.4, 2.2 and 2.9 cm), flow rate (5, 10 and 15 mL/min), influent Cr(VI) concentrations (100, 200 and 300 mg/L) and influent solution pH (2.66, 4.91 and 5.66) was investigated. The exhaustion time increased with increase of bed depth, decrease of flow rate and influent concentration. The Adams–Bohart, Thomas and Yoon–Nelson models were applied to the adsorption under varying experimental conditions to predict the breakthrough curves and to evaluate the model parameters of the fixed-bed column that are useful for process design. The Thomas and Yoon–Nelson models were in good agreement with the experimental data. The MCS column study states the value of the excellent adsorption capacity for the removal of Cr(VI) from aqueous solution.

Removal of Cr(VI) Ions from aqueous solutions using Poly 3-Methyl Thiophene Conducting Electroactive Polymers was studied by Reza Ansari et al.[68]. Their paper deals with a new application of poly 3-methyl thiophene synthesized chemically onto sawdust (termed as P3MTh/SD) as an effective adsorbent for removal of Cr(VI) ions from aqueous solutions using column system. Chemical synthesis of poly 3-methyl thiophene was performed by addition of ferric chloride (in chloroform) as oxidant to sawdust which had previously been soaked in monomer solution. All the sorption experiments were conducted using dynamic or column system at room temperature. The effect of important parameters such as pH and initial concentration on uptake of Cr(VI) was investigated. In order to find out the possibility of the regeneration and reuse of the exhausted adsorbent, desorption studies were also performed. The currently introduced adsorbent was found to be an efficient adsorbent for removal of highly toxic and hazardous Cr(VI) ions from aqueous solutions. As their breakthrough analysis has indicated, each gram of P3MTh/SD is able to remove more than 95% of Cr(VI) ions from 300 mL of Cr(VI) polluted solution with the initial concentration of 25 mg l<sup>-1</sup> in column system. Sorption/desorption of Cr(VI) ions was found to be a highly pH dependent processes.

Kinetics and thermodynamics of Cr(VI) ion adsorption onto organo-bentonite from the Amazon region was studied by D. J. L. Guerra et al.[69]. A natural bentonite clay sample from the Amazon region (Amazonas State) was utilized for the synthesis of new hybrid materials (organo-bentonite) produced by the organofunctionalization process. The organo-bentonite types were composed of an Amazon bentonite sample, 3-aminopropyltriethoxysilane and 3,2-aminoethylaminopropyltrimethoxysilane. The natural bentonite and organo-bentonite samples were used in batch studies for the adsorption of Cr(VI) ions from aqueous solution. The adsorption data were fitted to equilibrium and kinetic models. The effects of stirring time, adsorbent dosage and pH on the adsorption capacity demonstrated that 90 min is sufficient to reach equilibrium at room temperature and over a pH range of 6.0–8.0, the batch results were

confirmed by column method and show that the adsorption process of materials accorded with Redlich–Peterson, Sips, and Langmuir isotherm models. The exothermic enthalpic values reflected a favorable energetic process for chromium ions anchored in the material surfaces. The negative Gibbs free energy results supported the spontaneity of three adsorption reactions with Cr(VI) ions. The model of Adams–Bohart was used to analyze the adsorption experimental data and the model parameters were evaluated.

Performance evaluation of fixed bed of Nano calcium oxide synthesized from a gastropod Shell (*Achatina achatina*) in Hexavalent Chromium Adsorption from Aqua System was studied by N. A. Oladoja et al.[7]. The shell of a gastropod (*Achatina Achatina*) was used as a precursor for the synthesis of nano calcium oxide (NC) via the sol–gel technique. The NC was characterized and the performance evaluation in chromium (Cr) (VI) adsorption was assessed in a fixed bed. The operating characteristics of the NC-Cr (VI) system were analysed with the mass transfer model and the mass transfer zone parameters were found to fluctuate with changes in the initial Cr (VI) concentration. The evaluation of the equilibrium data, generated from the fixed bed studies, showed that the sorption of Cr (VI) occurred via monolayer adsorption mechanism, and the monolayer sorption capacity was 833.33 mg/g. Different kinetic models (i.e., Adams–Bohart, Thomas, Wolborska, and Yoon–Nelson models) were applied to experimental data to predict the breakthrough curves and to determine the parameters of the column useful for process design. The kinetic analysis showed that the Yoon and Nelson model had the best fitting of the experimental data. The data obtained for Cr (VI) removal, when the NC bed height was optimized, were well described by bed depth service time model.

Biosorption of Cr(VI) from aqueous solution using *A. hydrophila* in up-flow column was studied by S. H. Hasan et al.[70]. In their study, continuous up-flow fixed bed column study was carried out using immobilized dead biomass of *Aeromonas hydrophila* for the removal of Cr (VI) from aqueous solution. Different polymeric matrices were used to immobilized biomass and polysulfone-immobilized biomass has shown to give maximum removal. The sorption capacity of immobilized biomass for the removal of Cr(VI) evaluating the breakthrough curves obtained at different flow rate and bed height. A maximum of 78.58% Cr(VI) removal was obtained at bed height of 19 cm and flow rate of 2 mL/min. Bed depth service time model provides a good description of experimental results with high correlation coefficient ( $>0.996$ ). An attempt has been made to investigate the individual as well as cumulative effect of the process variables and to optimize the process conditions for the maximum removal of chromium from water by two-level two-factor full-factorial central composite design with the help of Minitab ® version 15 statistical software. The predicted results are having a good agreement ( $R^2=98.19\%$ ) with the result obtained. Sorption–desorption studies revealed that polysulfone-immobilized biomass could be reused up to 11 cycles and bed was completely exhausted after 28 cycles.

Adsorption of Cr(VI) on 1,2-ethylenediamine-aminated macroporous polystyrene particles was studied by Lili Cui et al.[71]. An adsorbent, 1,2-ethylenediamine-aminated macroporous polystyrene (EDA-PSt) particles was used to adsorb Cr(VI) from aqueous solution. Effect of pH value, contact time, temperature, adsorbent dosage and initial Cr(VI) concentration on adsorption amount of Cr(VI) on EDA-PSt were investigated. The results showed that the adsorption isotherm can be well described by the Langmuir equation and the adsorption kinetics fitted to the pseudo-second-order model. According to Langmuir equation,  $Q_m$  was calculated to be 175.75 mg g<sup>-1</sup>. The breakthrough curve experiment showed that the dynamic adsorption capacity for Cr(VI) on EDA-PSt was 100.06 mg g<sup>-1</sup>. The adsorbed Cr(VI) could be desorbed by 0.1 mol L<sup>-1</sup> NaOH and the desorption ratio was 67.28%.

Sorption of metal ions from aqueous solution on fixed-beds of iron-based adsorbents was studied by E.A. Deliyanni et al.[72]. The possibility of using a packed-bed in column configuration of akaganéite or goethite to remove metal ions (like zinc, cadmium, arsenates and chromates) from aqueous solutions was the aim of the present review paper. Synthesized material was used in two forms, i.e. in fine powder of nanocrystals and in the form of grains (as granular). The main examined parameters were the quantity of sorbent in the column, the presence of ionic strength, the solution pH value and the metals speciation, including the presence of complexing agents. The removal efficiency of the column was examined and compared. Typical adsorption models were discussed and the bed depth – service time equation has been applied to the sorption results in order to model the column operation.

Experimental Investigations and Theoretical Modeling Aspects in Column Studies for Removal of Cr(VI) from Aqueous Solutions Using Activated Tamarind Seeds was studied by Suresh Gupta et al.[73]. Continuous adsorption experiments are conducted using fixed-bed adsorption column to evaluate the performance of the adsorbent developed (from activated tamarind seeds) for the removal of Cr(VI) from aqueous solutions and the results obtained are validated with a model developed in this study. The effects of significant parameters such as flow rate, mass of adsorbent, and initial Cr(VI) concentration are studied and breakthrough curves are obtained. As the flow rate increases from 10 to 20 mL min<sup>-1</sup>, the breakthrough time decreases from 210 to 80 min. As the mass of adsorbent increases, breakthrough time get delayed. The breakthrough times were obtained as 110, 115 and 210 min for 15, 20 and 25 g of activated tamarind seeds. As the initial Cr(VI) concentration increases from 100 to 200 mgL<sup>-1</sup>, the break point time decreases from 210 to 45 min. The process parameters for fixed-bed adsorption such as breakthrough time, total percentage re-moval of Cr(VI), adsorption exhaustion rate and fraction of unused bed length are calculated and the performance of fixed-bed adsorption column was analyzed. The mechanism for Cr(VI) adsorption on activated tamarind seeds was proposed. At low value of solution pH (= 1), the increase in Cr(VI) adsorption is due to the electrostatic attraction between positively charged groups of activated tamarind seeds and the HCrO<sup>4-</sup>. A mathematical model for fixed-bed adsorption column is proposed by incorporating the effect of velocity variation along

the bed length in the existing model. Pore and surface diffusion models are used to describe the intra-particle mechanism for Cr(VI) adsorption. The breakthrough curve obtained theoretically from pore diffusion model and surface diffusion model are compared with experimental results for different operating conditions. The standard deviation values obtained for pore diffusion model and solid diffusion model are 0.111 and 0.214 respectively.

Removal of chromium ions from synthetic industrial wastewater using continuous ion exchange column system was studied by Bilal Saeed Mahyoub Ahmed.[74]. The removal of two types of chromium ions i.e. Cr (III) and Cr (VI) from synthetic wastewater solution using a cation exchange resin (AMBERLITE 200) was studied under a dynamic condition in a fixed bed column system. Three different solutions were used during this study containing Cr (III), Cr (VI) solution and mixture of metals including Cr(III),Cr(VI), Cd(II) and Cu(III) ions. The response surface methodology used for experimental design the data and to evaluate the effect of the operating parameters such as initial concentration, bed height, and flow rate on the performance of removal of the heavy metal ions. The performance of the system was evaluated in terms of percentage of heavy metal removal and breakthrough curve. Space velocity and distribution coefficient were also determined in order to evaluate the efficiency of the ion exchange resin in removing Cr(III) and Cr(VI) from synthetic wastewater. From the response surface plots and breakthrough curves, it was found that the ion exchange resin efficiency and its breakthrough time were increased with decrease in the initial concentration and the flow rate. It also increased with increases in bed height. Equilibrium distribution coefficient,  $K_d$  of Cr(III) and Cr(VI) indicated that AMBERLITE 200 was more selective for Cr(III) than for Cr(VI). The overall results suggest that the resin (AMBERLITE 200) has high efficiency of in the removal of Cr(III) than Cr(VI), with the percentage removal of Cr(III) is in the range of 92%-99% and that for Cr(VI) is in the range of 30%-70%.

The Study of Adsorption Breakthrough Curves of Cr(VI) on Bagasse Fly Ash (BFA) was studied by Chandra W. Purnomo et al.[75]. The breakthrough curves of Cr(VI) on bagasse fly ash (BFA) at room temperature were measured in a fixed-bed apparatus. It has been tried to fit the experimental data to fixed-bed model for breakthrough curve. Then, the effective diffusivity of hexavalent chrome ion was obtained. The effective diffusivity can be used to predict breakthrough curves at other adsorption conditions. The material characterizations have been conducted before the adsorption experiments.

Column study on the sorption of Cr(VI) using quaternized rice hulls was studied by K.S. Low et al.[76]. The potential of quaternized rice hulls in removing Cr(VI) from synthetic solution, chrome electroplating waste and wood preservative waste was investigated in column experiments. Increase in column bed depth resulted in a longer service time at  $C_t/C_o = 0.5$  breakthrough. The presence of  $SO_4^{2-}$ , which is commonly present in the wastes, interfered with

the sorption process and resulted in earlier breakthrough. The sorption process was flow-rate independent within the scope of this study. In the regeneration study, Cr(VI) could be recovered almost quantitatively by eluting with a 0.5 M NaOH solution and the column could be used repeatedly for at least five cycles.

Cr(VI) adsorption by waste acorn of *Quercus ithaburensis* in fixed beds was studied by Emine Malkoc et al.[77]. The adsorption of Cr(VI) onto waste acorn of *Quercus ithaburensis* was studied using fixed-bed adsorption. The experiments were conducted to study the effect of important design parameters such as flow rate, solution pH and particle size of adsorbent. Decrease in adsorbent particle size and flow rate produced a better bed capacity. Also an increase in flow rate and particle size resulted in a decrease in the bed volumes at the breakthrough. The highest bed capacities of fixed-bed column were obtained at pH 2.0. In the beginning of all the pH experiments, the effluent pH increased dramatically and then dropped and approached lower values. The breakthrough data obtained for Cr(VI) was adequately described by the Thomas and Yoon–Nelson adsorption models. Good agreement between the predicted theoretical breakthrough curves and the experimental results were observed. Their study indicated that the waste acorn of *Quercus ithaburensis* can be used as an effective and environmentally friendly adsorbent for the treatment of Cr(VI) containing wastewaters.

Ion exchange and adsorption fixed bed operations for wastewater treatment was studied by Inglezakis J. Vassilis.[78]. In part I of the study the theoretical models and hydraulics of fixed bed operations are presented. In part II the issues of scale-up and approximate design methods are presented. Part II could be considered as a presentation of the path from the laboratory scale to full scale units. Finally, the methods for derivation of the experimental data needed are discussed.

Fixed bed studies for the sorption of chromium(VI) onto tea factory waste was studied by Emine Malkoc et al.[79]. The adsorption of Cr(VI) ions from aqueous solutions onto waste of tea factory in fixed beds was investigated. Experiments were carried out as a function of liquid flow rate, initial feed of Cr(VI) concentration, particle size, feed solution pH and bed depth. The bed capacities were found to increase with decreasing flow rate and particle size. The maximum bed capacities for the tested flow rates were found to be 55.65, 40.41 and 33.71 mg g<sup>-1</sup> at 5, 10 and 20 ml min<sup>-1</sup>, respectively. When the initial Cr(VI) concentration was increased from 50 to 200 mg l<sup>-1</sup>, the corresponding adsorption bed capacity appears to increase from 27.67 to 43.67 mg g<sup>-1</sup>. The longest breakthrough time and maximum of Cr(VI) adsorption was obtained at the lowest examined pH value. Decrease in the particle size from 1.00–3.00 to 0.15–0.25mm resulted in significant increase in the treated volume, breakthrough time and bed capacity. Breakthrough volume varies with bed depth and the treated volume considerably increases from about 4200 to 11 800 ml as the bed depth increases from 5 to 30 cm. Thomas model for tea factory waste on Cr(VI) adsorption was used to predict the breakthrough curves under varying

experimental conditions. Their study indicated that the tea factory waste can be used as an effective and environmentally friendly adsorbent for the treatment of Cr(VI) ions in aqueous solutions.

Modeling and evaluation on removal of hexavalent chromium from aqueous systems using fixed bed column was studied by Divya Chauhan et al.[80]. Removal of hexavalent chromium by xanthated chitosan was investigated in a packed bed up-flow column. The experiments were conducted to study the effect of important design parameters such as bed height and flow rate. At a bed height of 20cm and flow rate of  $5\text{mL min}^{-1}$ , the metal-uptake capacity of xanthated chitosan and plain chitosan flakes for hexavalent chromium was found to be 202.5 and  $130.12\text{mg g}^{-1}$  respectively. The bed depth service time (BDST) model was used to analyze the experimental data. The computed sorption capacity per unit bed volume ( $N_0$ ) was  $4.6\pm 0.3$  and  $78.3\pm 2.9\text{gL}^{-1}$  for plain and xanthated flakes respectively at 10% breakthrough concentration. The rate constant ( $K_a$ ) was recorded as 0.0507 and  $0.0194\text{Lmg}^{-1}\text{h}^{-1}$  for plain and xanthated chitosan respectively. In flow rate experiments, the results confirmed that the metal uptake capacity and the metal removal efficiency of plain and xanthated chitosan decreased with increasing flow rate. The Thomas model was used to fit the column sorption data at different flow rates and model constants were evaluated. The column was successfully applied for the removal of hexavalent chromium from electroplating wastewater. Five hundred bed volumes of electroplating wastewater were treated in column experiments using this adsorbent, reducing the concentrations of hexavalent chromium from  $10\text{mgL}^{-1}$  to  $0.1\text{mgL}^{-1}$ .

Chromium uptake from tricomponent solution in zeolite fixed bed was studied by M. A. S. D. Barros et al.[81]. Removal of  $\text{Cr}^{3+}$ ,  $\text{Ca}^{2+}$ ,  $\text{Mg}^{2+}$  and  $\text{K}^+$  in equilibrium isotherms and in tricomponent solutions (Cr/Ca/K, Cr/Ca/Mg and Cr/Mg/K) were investigated in NaX and NaY packed beds at  $30^\circ\text{C}$ . The equilibrium selectivity was obtained as  $\text{Cr}^{3+} > \text{Mg}^{2+} > \text{Ca}^{2+} \approx \text{K}^+$  for zeolite NaY and  $\text{Ca}^{2+} \gg \text{Cr}^{3+} > \text{Mg}^{2+} \approx \text{K}^+$  for zeolite NaX. The breakthrough curves showed sequential ion exchange where chromium ions are able to replace the competing cations. Some mass transfer parameters, such as length of unused bed and overall mass transfer coefficient, were investigated. Chromium retention was also investigated through a mass balance. Based on the breakthrough results, it was concluded that chromium-uptake mechanism was hardly influenced by the competition and interaction between the entering ions. NaY showed a higher affinity towards  $\text{Cr}^{3+}$  for both equilibrium and dynamic systems and its sites were more efficiently used in the ion exchange process. Chromium was less retained in NaX due to the high selectivity towards calcium ions.

Kinetics and mechanism of adsorption of Cr (VI) by treated weed *Salvinia cucullata* was studied by Saroj S. Baral et al.[82]. In their study a new low cost, easily available and environmentally friendly adsorbent was used for removal of Cr (VI). The Cr (VI) removal efficiency of the adsorbent was studied as a function of contact time, pH, adsorbent dose, adsorbate concentration,

temperature and stirring speed. Different adsorption model equations for kinetics, isotherm and rate mechanism of the process were used to find the best model, which fit well to the experimental data. A full factorial design of  $n^k$  type was used to find a mathematical relation between the percentage of adsorption and variables affecting the adsorption process such as time, pH, adsorbate concentration and temperature. Using the Students't' test, the significance of each term of the derived equation was tested. The insignificant terms were removed from the derived equation. The adequacy of the equation after removing the insignificant terms was tested using the Fisher adequacy test. From the factorial design analysis it was found that pH has the most pronounced effect followed by time, temperature and the adsorbate concentration. A column study was performed using the optimum operating conditions.

Column sorption of Cr(VI) from electroplating effluent using formaldehyde cross-linked *Saccharomyces cerevisiae* was studied by Ming Zhao et al.[83]. Pellets of *Saccharomyces cerevisiae*, cross-linked by 13 % (w/v) formaldehyde, were used in fixed-bed columns to remove Cr(VI) from electroplating rinse effluent at varied influent pHs (2.5–7.5). The Cr uptake at 60 % saturation of the biomass was 6.3 mg/g at an optimum pH of 2.5. Desorption of the bound metal was partially achieved by washing the column biomass with a combined solution of 1 % (w/v) formaldehyde and 1 M HNO<sub>3</sub>.

Sorption of Cr(VI) on the Anion-Exchange Fibrous Material Based on Nitron was studied by D. A. Gafurova et al.[84]. The kinetics and thermodynamics of Cr(VI) sorption under the static and dynamic conditions on the fibrous sorbent SMA-1 prepared by chemical modification of polyacrylonitrile were studied.

### **Aim of the work:**

Ion exchange is gaining popularity due to the advantages of the process (long life of resins, cheap maintenance, and very low running costs). In addition, the process is very environmentally friendly because it deals only with substances already occurring in water.

The aim of the present study is to investigate the performance of Diaion SA20A, a strong anion exchange resin in Cr(VI) removal from synthetic wastewater. To this end, batch experiments have been conducted first to investigate equilibrium isotherm (such as: Langmuir, Freundlich and Temkin) and kinetics behavior (such as: pseudo first order, pseudo second order and Elovich) of the present resin in relation to the following parameters:

- i. pH of Cr(VI) Solution,
- ii. Contact time,
- iii. Initial concentration of hexavalent chromium ions,
- iv. rpm,
- v. The amount of resin and
- vi. Temperature.

In addition continuous experiments have been conducted using fixed-bed adsorption column to construct breakthrough curves under the following different parameters

- i. flow rate
- ii. bed height (mass of adsorbent)

The breakthrough curves for the adsorption of Cr(VI) have been analyzed using mathematical models, such as :Adams–Bohart, Thomas, Yoon–Nelson and BDST.